OKLAHOMA TRANSPORTATION CENTER

ECONOMIC ENHANCEMENT THROUGH INFRASTRUCTURE STEWARDSHIP

DEVELOPMENT OF A STRUCTURAL HEALTH MONITORING (SHM) GUIDEBOOK FOR CRITICAL BRIDGE STRUCTURES

ZHENYU (JAMES) KONG, PH.D.
TYLER LEY, PH.D., P.E.
TIEMING LIU, PH.D.

OTCREOS9.1-29-F

Oklahoma Transportation Center
2601 Liberty Parkway, Suite 110
Midwest City, Oklahoma 73110

Phone: 405.732.6580
Fax: 405.732.6586
www.oktc.org

DISCLAIMER

The contents of this report reflect the views of the authors, who are responsible for the facts and accuracy of the information presented herein. This document is disseminated under the sponsorship of the Department of Transportation University Transportation Centers Program, in the interest of information exchange. The U.S. Government assumes no liability for the contents or use thereof.

TECHNICAL REPORT DOCUMENTATION PAGE

1. REPORT NO.	2. GOVERNMENT ACCESSION NO.	3. RECIPIENT'S CATALOG NO.
OTCREOS9.1-29-F		

4. TITLE AND SUBTITLE	5. REPORT DATE
Development of a Structural Health Monitoring (SHM) Guidebook for Critical Bridge Structures	July 18, 2013
	6. PERFORMING ORGANIZATION CODE

7. AUTHOR(S)	8. PERFOMING ORGANIZATION REPORT
Zhenyu (James) Kong, Tyler Ley, and Tieming Liu	

9. PERFORMING ORGANIZATION NAME AND ADDRESS	10. WORK UNIT NO.
Oklahoma State University, School of Industrial Engineering & Management, 322 Engineering North, Stillwater OK 74078	11. CONTRACT OR GRANT NO. DTRT06-G-0016

12. SPONSORING AGENCY NAME AND ADDRESS	13. TYPE OF REPORT AND PERIOD COVERED
Oklahoma Transportation Center (OkTC) (Fiscal) 201 ATRC, Stillwater, OK 74078 (Technical) 2601 Liberty Parkway, Suite 110 Midwest City, Oklahoma 73110	Final report: June 1, 2009 – Dec. 31, 2012
	14. SPONSORING AGENCY CODE

15. SUPPLEMENTARY NOTES

University Transportation Center

16. ABSTRACT

A recently completed study suggests that approximately 25% of them are either structurally deficient or functionally obsolete (FHWA, 2007). Therefore, the Federal Highway Administration (FHWA) and the Oklahoma Transportation Center (OTC) have made it a priority to seek new methods to economically and effectively inspect and monitor bridges. In response to this need, structural health monitoring (SHM) has been developed for bridge inspection and monitoring. However, implementation of SHM on bridges is not common because of the following challenges: (1) difficulties in integration of the information from sensor networks, (2) economic justification of SHM for the structure, and (3) the lack of a standard procedure for owners and inspectors to follow for SHM of bridges. To address these challenges, the overall objective for this project is to produce some guides for owners and design engineers to inform and assist them in deciding when SHM is useful. The following research tasks are reported in this document: (1) Conduct case studies of bridge inspection using SHM systems based on previous sensor networks used by the industrial partner and provide suggestions for hybrid sensor networks, (2) Develop a guideline for using analysis techniques (e.g., finite element analysis) as a screening tool to determine the most critical areas of the structural system, (3) Establish methods for determining types/numbers/locations of sensors to be used to study the performance of the structure, and (4) Create tools using statistical analysis and signal processing for analyzing the data from the SHM system when making repair decisions.

17. KEY WORDS	18. DISTRIBUTION STATEMENT
Structural health monitoring, damage detection, optimal sensor palcement	No restrictions. This publication is available at www.oktc.org.

19. SECURITY CLASSIF. (OF THIS REPORT)	20. SECURITY CLASSIF. (OF THIS PAGE)	21. NO. OF PAGES	22. PRICE
Unclassified	Unclassified	63 + covers	

SI (METRIC) CONVERSION FACTORS

Approximate Conversions to SI Units

Symbol	When you know	Multiply by	To Find	Symbol
	LENGTH			
in	inches	25.40	millimeters	mm
ft	feet	0.3048	meters	m
yd	yards	0.9144	meters	m
mi	miles	1.609	kilometers	km
	AREA			
in^2	square inches	645.2	square millimeters	mm
ft^2	square feet	0.0929	square meters	m^2
yd^2	square yards	0.8361	square meters	m^2
ac	acres	0.4047	hectares	ha
mi^2	square miles	2.590	square kilometers	km^2
	VOLUME			
fl oz	fluid ounces	29.57	milliliters	mL
gal	gallons	3.785	liters	L
ft^3	cubic feet	0.0283	cubic meters	m^3
yd^3	cubic yards	0.7645	cubic meters	m^3
	MASS			
oz	ounces	28.35	grams	g
lb	pounds	0.4536	kilograms	kg
T	short tons (2000 lb)	0.907	megagrams	Mg
	TEMPERATURE (exact)			
°F	degrees Fahrenheit	(°F-32)/1.8	degrees Celsius	°C
	FORCE and PRESSURE or STRESS			
lbf	poundforce	4.448	Newtons	N
lbf/in^2	poundforce per square inch	6.895	kilopascals	kPa

Approximate Conversions from SI Units

Symbol	When you know	Multiply by	To Find	Symbol
	LENGTH			
mm	millimeters	0.0394	inches	in
m	meters	3.281	feet	ft
m	meters	1.094	yards	yd
km	kilometers	0.6214	miles	mi
	AREA			
mm^2	square millimeters	0.00155	square inches	in^2
m^2	square meters	10.764	square feet	ft^2
m^2	square meters	1.196	square yards	yd^2
ha	hectares	2.471	acres	ac
km^2	square kilometers	0.3861	square miles	mi^2
	VOLUME			
mL	milliliters	0.0338	fluid ounces	fl oz
L	liters	0.2642	gallons	gal
m^3	cubic meters	35.315	cubic feet	ft^3
m^3	cubic meters	1.308	cubic yards	yd^3
	MASS			
g	grams	0.0353	ounces	oz
kg	kilograms	2.205	pounds	lb
Mg	megagrams	1.1023	short tons (2000 lb)	T
	TEMPERATURE (exact)			
°C	degrees Celsius	9/5+32	degrees Fahrenheit	°F
	FORCE and PRESSURE or STRESS			
N	Newtons	0.2248	poundforce	lbf
kPa	kilopascals	0.1450	poundforce per square inch	lbf/in^2

ACKNOWLEDGMENTS

The investigators would like to express their gratitude for the OTCREOS9.1-29 grant from the Oklahoma Transportation Center (OkTC) that enabled us to conduct this research.

The investigators would like to thank the following graduate research assistants for their hard work and contributions: Mr. Eyosias Beneberu, Mr. Ermias Biru, Mr. Philipose Tewolde, and Mr. Mahmoud Mistarihi.

The research team would also like to acknowledge the support of their respective proposal services, grants administration and departmental staff.

Development of a Structural Health Monitoring (SHM) Guidebook for Critical Bridge Structures

Final Report

July 2013

Zhenyu (James) Kong, Ph.D., School of Industrial Engineering and Management

Tyler Ley, Ph.D., P.E., School of Civil and Environmental Engineering

Tieming Liu, Ph.D., School of Industrial Engineering and Management

Oklahoma State University

Oklahoma Transportation Center (OkTC)

2601 Liberty Parkway, Suite 110

Midwest City, Oklahoma 73110

TABLE OF CONTENTS

LIST OF FIGURES

LIST OF TABLES

EXECUTIVE SUMMARY

In order to effectively inspect and monitor the conditions of bridges, structural health monitoring (SHM) has become a very important research topic for both industry and academia. If properly implemented, SHM will allow owners to extend the useful life of bridges by allowing deteriorations/damages to be identified before major repairs are required. The overall objective for this project is to produce some guide for owners and design engineers to inform and assist them in deciding how to apply SHM related technologies. To focus on this objective, the following specific research tasks have been successfully carried out with some promising results.

(1) **Case studies for SHM of bridges**: 40 different case studies of the use of structural health monitoring for different types of transportation infrastructure have been compiled and summarized. These case studies are useful for providing some guides for civil engineers with respect to what kind of sensors and analysis tools could be chosen for different types of bridges.

(2) **Critical damages identification of bridges using Finite Element Modeling**: This task is focused on the structural modeling of a bridge using finite element modeling. Two simplified computational models have been developed to confirm the capability of replicating a field load test. These models can also be used to identify critical areas on these bridges to determine potential locations for sensor placement in a structural health monitoring.

(3) **Optimal sensor placement for Structural Health Monitoring**: The basic methodology and procedure for bridge sensor network are investigated. This task formulates the optimal criteria of the sensor placement for damage detection problem based upon a partial differential equation (PDE) analytical model. The study results show that the proposed optimal sensor placement method minimizes the uncertainty in the estimated model parameters, leading to reduced number of sensors and improved detection rate for structural damages.

(4) **Application of advanced statistical analysis and signal process techniques**: (a) Various data analysis tools are applied, among which Empirical Mode

Decomposition (EMD) and Hilbert Huang Transform (HHT) show their superior performance for early damage detection; (b) The proposed damage detection algorithm using correlation dimension makes the online monitoring of nonlinear/nonstationary processes more applicable and efficient; and (c) the proposed empirical mode decomposition method for online damage prediction has obtained significant prediction accuracy improvement over other commonly used prediction techniques.

1. Introduction

The United States has approximately 600,000 highway bridges that are the lifelines of economic commerce (ASCE, 2009). A recently completed study suggests that approximately 25% of them are either structurally deficient or functionally obsolete (FHWA, 2007). The condition of these bridges poses a threat to public safety and local economies. The bridges in Oklahoma and across the nation are in dire need of improvement and the associated costs are overwhelming. A $17 billion annual investment is estimated by ASCE to be needed to improve current bridge conditions (ASCE, 2009). Therefore, the Federal Highway Administration (FHWA) and the Oklahoma Transportation Center (OTC) have made it a priority to seek new methods to economically and effectively inspect and monitor bridges.

In response to this need, structural health monitoring (SHM) has become a much discussed, but not widely implemented, topic. These techniques, if properly implemented, will allow owners to extend the useful life of bridges by allowing deterioration/damage to be identified early. This would allow corrective repairs or maintenance to be taken before the deterioration/damage grows to a condition where major repairs are required. Implementation of SHM on bridges is not common because of the following challenges: (1) difficulties in integration of the information from sensor networks, (2) economic justification of SHM for the structure, and (3) the lack of a standard procedure for owners and inspectors to follow for SHM of bridges.

To address these challenges, the overall objective for this project is to produce a practical, economically minded, and easily implementable guide for owners and design engineers to inform and assist them in deciding when SHM is useful. This guide will be focused on providing SHM guidance for large or critical bridge structures that serve as major lifelines for communities as these structures are currently the most economically justifiable to fit with SHM instruments. The following topics will be covered in the guide book: (i) case studies with descriptions of which sensor networks have been shown to be successful, (ii) the optimal location and number of sensors to monitor structural health, and (iii) guidelines for analyzing and interpreting data obtained by the SHM

system. To help focus these objectives, the following specific research tasks have been successfully carried out,

(1) Conduct case studies of bridge inspection using SHM systems based on previous sensor networks used by the industrial partner and provide suggestions for hybrid sensor networks,
(2) Develop a guideline for using analysis techniques (e.g., finite element analysis) as a screening tool to determine the most critical areas of the structural system,
(3) Establish methods for determining types/numbers/locations of sensors to be used to study the performance of the structure, and
(4) Create tools using statistical analysis and signal processing for analyzing the data from the SHM system when making repair decisions.

The above four research tasks are introduced in details through Section 2 to Section 5, respectively. Finally, the summary and conclusion are provided in Section 6.

2. Investigation in Case Studies of Actual Bridge SHM Systems

In this task, 40 different case studies of the use of structural health monitoring for different types of transportation infrastructure have been collected, compiled, and summarized. These case studies are used to develop a guide book for civil engineers to provide some help with respect to what kind of sensor and analysis tools could be chosen for different types of bridges. For each bridge, the following questions are investigated and answered:

(1) General information about the bridge;
(2) Types of sensor used and measured parameters;
(3) What are the key areas of measurement?
(4) What utilities are available?
(5) What accuracy is needed in the measurement?
(6) What rate of readings is needed?
(7) How will the data be retrieved?
(8) How was the data processed? and
(9) What challenges did the project have?

2.1 An example out of 40 case studies conducted

An example out of the 40 case studied is introduced below to describe some basic principles for structural health monitoring,

1. *General information about the bridge* (Bridge Engineering Center, 2006):

- Name: The east 12th street Bridge over I-235 (see Fig. 2.1)
- Location: Des Moines, Iowa
- Span : The north span is 153 ft long while south span is 145 feet long
- Type : High performance steel girder bridge

2. *Types of sensor used and measured parameters*:

Fiber Bragg Grating (FBG) sensors are used to monitor strain.

Figure 2.1 The East 12th street Bridge, Des Moines, Iowa

3. *What are the key areas of measurement*?

A total of 40 sensors are used for this particular bridge. The FBG sensors are located at strategic point on the bridge such that both the local and global performance of the bridge can be assessed. The global performance is monitored with FBG sensors placed on the top and bottom flange of the girders at mid span of the north and south spans of the bridge. Top and bottom flange sensors are also placed at the north abutment and near the bridge pier. Local effects of traffic events are monitored at several locations. The web gap regions of several girders are instrumented near the pier. Stress concentration is also being monitored near the flange and web splices in the negative moment region at the pier. FBG sensors are also placed at the locations of the bridge to measure the steel temperature. These sensors are not attached to the bridge like other sensors. A final FBG sensor is placed in the protective cabinet that house Si425 – 500 (Si425 – 500 is the data acquisition subsystem located at the bridge) which allows the monitoring of the temperature in the cabinet.

4. *What utilities are Available*?

It used wireless internet for communication.

5. *What accuracy is needed in the measurement*?

The primary purpose of the SHM study on the bridge is to understand the long term effects of live load. Hence, elimination of temperature strain is performed to ensure the required accuracy in measurement of strain due to live load.

6. *What rate of readings is needed*?

Data is collected continuously. A website portal for the SHM system is developed to allow clients to view real-time video of traffic crossing the bridge and the corresponding real-time strain data at various bridge locations.

7. *How will the data be retrieved*?

The data acquisition subsystem (DASS) collects raw data from strain sensors strategically located on the bridge and transfer the information to the Gateway sub system (GSS), which is located approximately 450 feet from the bridge in a secured building. From the GSS, this data is distributed via the internet to the Iowa state university researchers and also to a website portal.

8. *How was the data processed*?

First elimination of temperature strain from the complete strain record, monitoring the global behavior of bridges and counting stress cycles is performed by Bridge engineering center (BEC) to ensure the entire system is operating properly. Second system check is performed that includes temperature of equipment, data continuity, transfer of all information, and minimum, maximum and average daily strain. And then elimination of temperature is performed to understand the long-term effects of live load on the bridge. After performing these steps the global behavior of the bridge is monitored by computing the distribution factors, neutral axis location and end restraint ratios.

9. *What Challenges did the project have*?

- Optical loss: Channel 1 consisted of 14 sensors. After all 14 sensors were installed, the system was powered on and only 13 gages responded. According to researchers one of the gages did not respond. Because when the temperature rose approximately 50 degrees above installation temperature of the channel, gage #14 is unrecognizable because of optical loss.

- Interference between sensors: This problem occurs when the wavelengths form two sensors are so close to each other.

- Large range sensors: Some of the sensors have experienced a large difference between daily maximum and minimum strains than other sensors. The ranges for these sensors have also increased since the system was installed. Some of the possible reasons are:
    - Chang in the global physical properties of the bridge;
    - Change in the local physical properties of the bridge;
    - Location of sensors are more susceptible to temperature change;
    - Localized effect on the sensor; and
    - Grating malfunction

- Large compressive change: Sensors that experienced a large range of daily strain, a large compressive change in strain was noticed. The sharp drop could due to:
    - Change in the physical properties of the bridge;
    - Change in the local physical properties of the bridge;
    - Localized effects on the gage; and
    - Grating malfunction

10. *How did the monitoring helps with the health of the structure*?

The SHM system installed at East 12th Street Bridge helps the owner to monitor and evaluate the performance of the bridge from a remote location. As a result it will help them decide to take remedial measures before the occurrence of serious damage.

2.2 Sensors used in SHM for bridges

Depending on what is required to be measured, sensors like Acoustic sensor, Global Positioning System (GPS), Elasto-Magnetic sensor, Fiber Optic sensor etc. are widely used in SHM for bridges.

Acoustic Sensors: Acoustic health monitoring is one type of monitoring system that is employed in post-tensioned building, pre stressed, cable supported roofs and several types of bridges including suspension bridge. It is primarily used to detect wire breakage in suspension bridge as the event happens. When one or more wire breaks the acoustic monitoring detects the release of energy. The energy releases from a wire breaks causes high frequency vibration to be sent up and down. A voltage is then created by the vibration as the sensors contain piezoelectric device. The voltage is sent to the data acquisition system (DAS) for analysis to detect wire breakage. The term “acoustic” implies the monitoring system uses sound to detect wire breakage. As a result it is highly likely for the sensors to recognize noises which are generated by other activities on the bridge rather than wire breakage. To solve this problem, the acoustic monitoring system is equipped to filter out and distinguish sound generated by the event of interest that is wire breakage.

Elasto-Magnetic Sensors: The Elasto-Magnetic (EM) sensor is a simple non-destructive evaluation technique for monitoring actual stress in tendons and cables based on the fact that the permeability of the ferromagnetic material is a function of magnetic history and applied field (stress and temperature). The cables in suspension/cable stayed bridge contain several hundreds of 7 mm diameter wires which are sheathed in a plastic protective cover filled with cement grout. For this reason strain gages which are used to measure pre stressed cables are impossible to use for suspension or cable stayed bridge. The Elasto-Magnetic sensor overcomes this problem in such a way that they can be integrated as a part of the tendon during its construction or installed on site at the existing tendons regardless of the size of the tendon. In addition to this, EM sensors are believed to have reliable accuracy, reasonable price, manageable and small size, and durable or lasts for longer time. The

time required for measurement is close real-time measurement and it can be applied to any structure built with circular steel reinforcements or cables.

***Global Positioning System* (*GPS*):** The GPS has been used for many years for deformation monitoring of structures such as buildings, bridges, dams, etc. Specifically for suspension bridges, it is used to measure the static three dimensional coordinates and the dynamic vertical displacement of the deck. Currently, GPS alone made it possible to measure the 3D deflections of discrete points upon a structure at a rate of up to 100 HZ. The rate of data acquisition can be increased up to 2000 Hz by integrating GPS with other types of sensors such as accelerometers. The GPS based deflection measurement has distinct advantages over other sensors in that GPS does not drift with precise time, and it can be used in various weather conditions. For the monitoring of suspension bridges, it is desirable for the measurement system to deliver equal precision in all position components, all the time. When using GPS, the accuracy, availability, reliability and integrity of the position solutions are very dependent on the number and geometric distribution of the available satellites. Therefore, the positioning precision is not the same in all three components, and large variations in positioning precision can be expected during a 24-hour period. This situation becomes worse when the line-of sight to GPS satellites becomes obstructed, such as in urban environments. To solve this problem Pseudolites can be used to augment GPS and improve a geometrically-weak satellite constellation.

3. Damages Identification Using Finite Element Modeling

The bridge considered in this study was modeled using structural analysis software according to their as-built conditions. As part of this study, a comparison of the results with the consideration of full stiffness and a 25% loss of stiffness in the interior girders of certain spans studied will help provide insight to the feasibility of the use of structural health monitoring (SHM) techniques. It is important to note, however, that any construction imperfections were not considered in the computational modeling of the bridge. The structural analysis software program STAAD Pro. 2007 was used to computationally model the bridge. The bridge was modeled in a fully three-dimensional environment capturing the entire three-dimensional response of the bridges to the given loading conditions. The details of the model as well as the load cases considered are discussed in the following sections.

3.1 Model building

The bridge is modeled in a fully three-dimension environmental to capture the resulting responses due to the loading conditions. The structure is divided into two primary components: (1) Superstructure and (2) Substructure. Both of these components together comprise the entirety of the bridge. However, one of the primary objectives of this study was to investigate the structural performance of the superstructure component of the bridge. Thus, Figure 3.1 shows the three-dimensional computational model of the bridge superstructure. The computational model considers the bridge substructure, part of the bridge consisting of those components related to the foundation, as infinitely stiff support because their performance is assumed not to adversely affect the performance of the super structure. Based on the construction specifications, these supports were modeled as simple supports (pin-roller combinations).

Since the bridge superstructure is the primary component of the bridge to be modeled, much of the investigation will be focused to that end. It would, however, be negligent to omit a discussion of the bridge substructure. Thus, both the bridge superstructure and substructure are further discussed as follows.

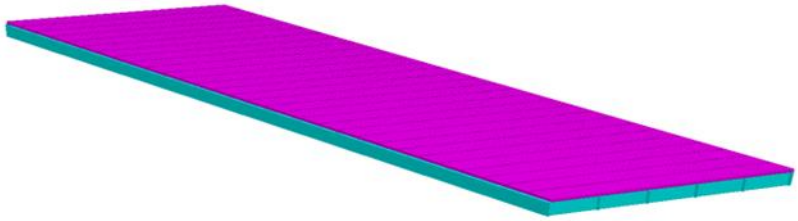

(a) View 1

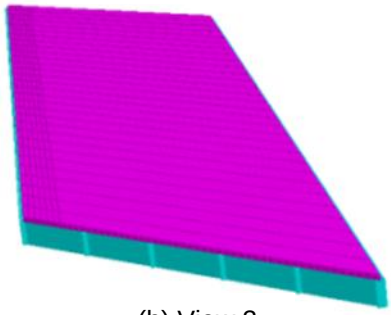

(b) View 2

Figure 3.1 Three Dimensional View of the Bridge

Superstructure: The bridge superstructure consists of those components of the bridge not related to the foundation. Such items include the bridge girders, diaphragms, and bridge deck. Other components in the superstructure, such as the parapets, are assumed to not contribute significantly to the stiffness of the structure. Figure 3.2 illustrates the girder and diaphragm layout for the bridge. Elements shown as rectangular blocks are concrete bridge girders and diaphragms. The bridge deck is overlaid on top of the girders and diaphragms.

Table 3.1 provides section properties for the girders, diaphragms, and bridge deck. The girders, diaphragms, and bridge deck are all composed of concrete. The details of the concrete girders are provided in Figure 3.3. On top of the concrete bridge deck is a 2-inch asphalt overlay. It is assumed that the bridge deck is acting compositely with the girders. Furthermore, it is also assumed that the bridge deck is continuous over the length of the bridge.

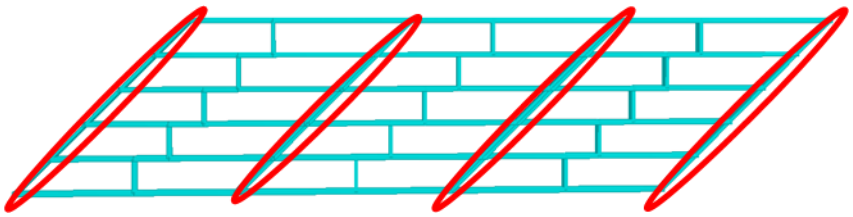

Figure 3.2 Bridge Girder Layout

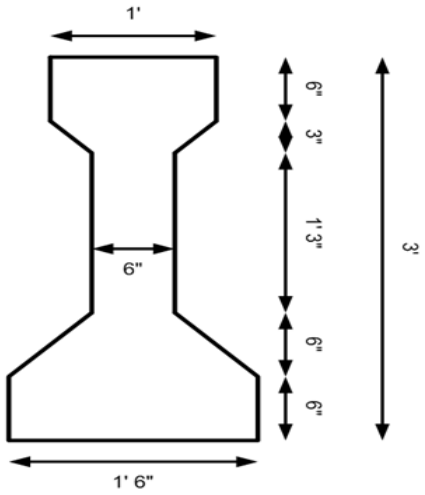

Figure 3.3 Bridge – Concrete Girder Section

Table 3.1 Bridge – Section Properties

Span	Members	Section	Material	Length
Left Span (Span 1)	All Girders (G1 – G6)	See Figure 4-19	Concrete	46 ft 9 in
Center Span (Span 2)	All Girders (G1 – G6)	See Figure 4-19	Concrete	45 ft
Right Span (Span 3)	All Girders (G1 – G6)	See Figure 4-19	Concrete	46 ft 9 in
All Spans (Spans 1, 2, and 3)	All Diaphragms	2.5 ft x 8 in Rect.	Concrete	7 ft 4 in
All Spans (Spans 1, 2, and 3)	Bridge Deck	Slab	Concrete	7 ½ in

Table 3.2 provides the material properties for the concrete components of the superstructure. These values were assumed ones provided by the material library in the structural analysis software.

Table 3.2 Bridge Material Properties

Categories	Properties
Material Type	Concrete
Elastic Modulus (E)	3,150 ksi
Poisson's Ration (*v*)	0.170
Density (ρ)	149.99 lb/ft^3

Substructure: The bridge substructure consists of those components of the bridge related to the foundation. Such items include the bridge abutments, pier foundations, pier caps, among others. These components, however, were not modeled in the computational model. Their performance is assumed to not adversely affect the performance of the superstructure. As such, the substructure was modeled as infinitely stiff supports. These supports are highlighted in Figure 3.2. The encircled areas, indicating the separation of the bridge spans, are locations of the bridge substructure. Based on the construction specifications, these supports were modeled as simple supports (pin-roller combinations).

3.2 Formulation for loading

The loading considered for the bridge is a truck loading idealized as a harmonic sinusoidal point load applied at the first natural frequency of the bridge. The amplitude of the load is taken as the total sum of the load from all the wheels of the truck shown in Figure 3.4.

The assumed truck loading was first placed at Node 266 in the first span of the bridge. Another loading condition was considered by placing the dynamic load at Node 266 on the first span and at Node 797 of the second span of the bridge simultaneously. As for the sign support structure, a change in the stiffness of the girders was considered to see the effect on the corresponding change in response of the superstructure. Therefore, two general cases are considered for the Loading as follows,

1) Dynamic Harmonic Loading applied on the first span alone, and
2) Dynamic Loading applied both on the first and second span of the bridge.

Apart from the general cases, two other cases were considered in each of the above general cases. The first loading condition is when keeping the bridge girder originally assumed properties as they are and the second case is when 25% of the assumed stiffness is lost due to crack, delamination, and other environmental conditions.

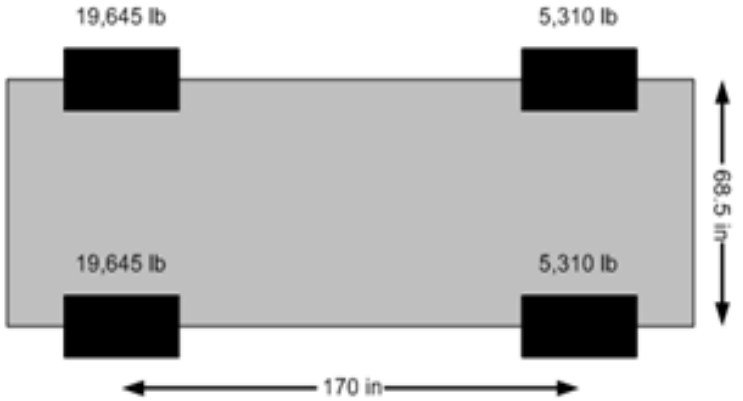

Figure 3.4 Bridge – Truck Loading

Harmonic Loading: The harmonic loading is formulated as following equation, $P=P_o \sin(\omega t)$, where P_o is amplitude of the harmonic loading assumed to be the total truck load acting at a point; ω is the natural frequency of the bridge structure; and t is time (second).

3.3 Response history plots

The response history of the bridge structure due to the applied harmonic load is given in Figure 3.5. All displacements are measured at a single node in the 1st span.

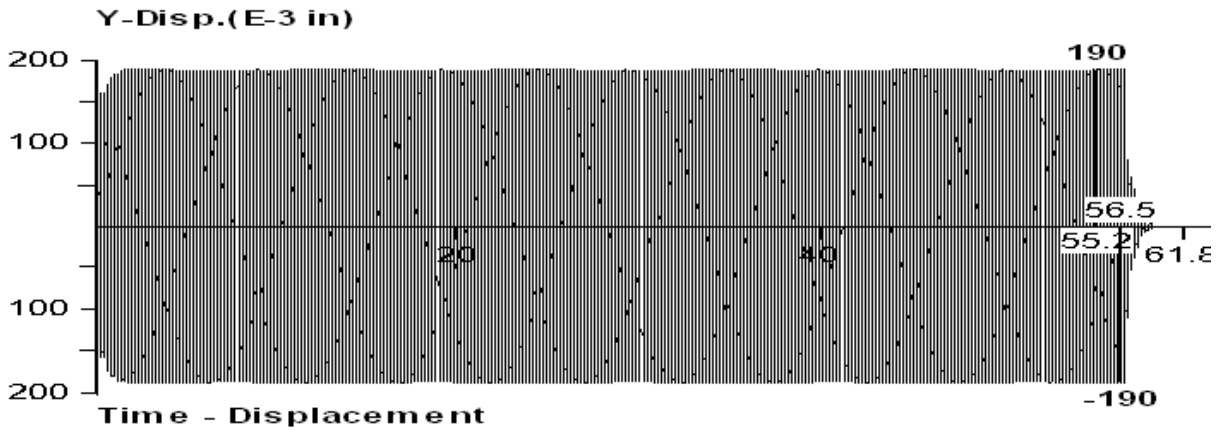

(a) Load Applied in the 1st Span

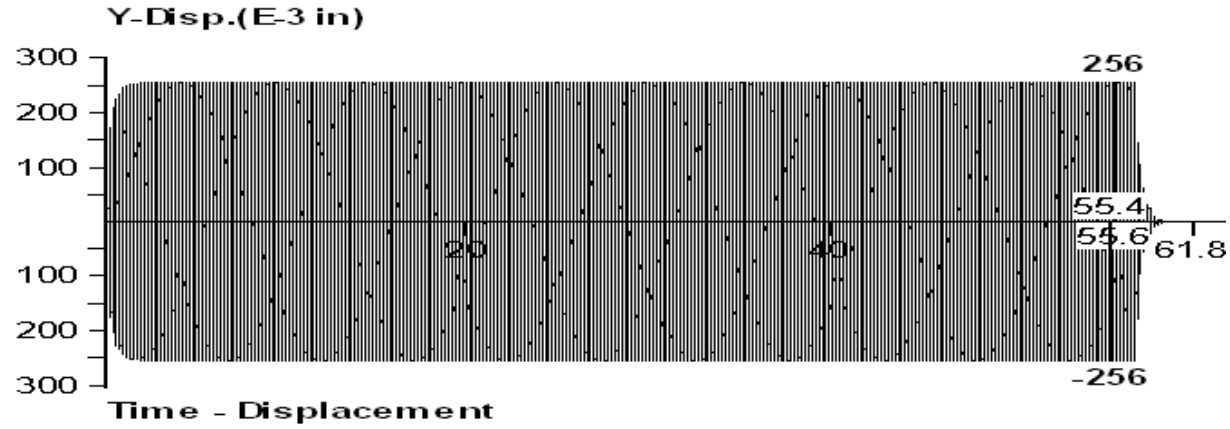

(b) Load Applied in the 1st Span with 25% Reduction in Interior Girder Stiffness

Figure 3.5 Time-History of Response of Bridge

3.4 Comparison of the results

We can observe from the static analysis that higher beam stresses occurred near the ground support of the pole and close to the connection between the pole and the cantilever arm of the cantilever part of the sign support structure. This will also give us a good indication on what type of sensor, location of the sensor, and how many sensors need to be installed for the structure studied. As can be seen from the response plots for displacement of the sign support structure, the responses were higher for the structure with the wall thickness of the pole near the support reduced by 50%. There is a slight difference between the responses of the original structure and the one with the cantilever wall thickness near the connection to pole reduced by 50%. A change in

response would have been better noticed if the length of the wall thickness change was increases from what is actually used in this model, which is 0.5 ft.

Comparing the responses of the bridge for the different cases considered, we can generally tell that when the stiffness of the interior beams is reduced, the responses get higher in value. We can also observe that the responses at the considered nodes that when the harmonic point load is applied only on the first span are higher than the responses when two harmonic loads are applied near the center of each span simultaneously. This can be attributed to other factors that might affect the response of the structure. In our case, the first span is longer than the middle span. Thus, we expect a higher response for a longer span length. Another reason can be that each harmonic load may have an adverse effect on the response of the other regardless of the nature of the forces (Sine or Cosine function of the harmonic load).

4. Sensor Network in Structural Health Monitoring

4.1 Procedures for sensor network design

The major phases for sensor network design in SHM should include sensor selection, power source, topology design, and sensor network optimization.

Phase 1 – Sensors and motes selection: there are many types of sensors and motes in the market for commercial and educational purposes. Appropriate sensors (and motes) should be suggested based on the spectacular characteristics of bridge structures and the types of structural health information to be monitored. The advantages and disadvantages of each type of sensors need to be studied. We list the sensors that could be used in SHM as follows:

- Strain gauges (including electrical resistance strain gauges, vibrating wire strain gauges, and fiber optic strain gauges).
- Displacement and position measurements (including cable extension transducers, linear variable differential transformers, vibrating wire crack meter, fiber optic displacement sensors, and global positioning system).
- Temperature measurements (including thermocouples and thermistors).
- Tilt measurement (vibrating wire tilt meter).
- Corrosion sensors.
- Accelerometers (Piezoresistive accelerometer).

Phase 2 – Power source selection: Sensors need power sources to monitor the structural health and communicate with the network. Sensors can be fed by batteries, direct power source from motes, solar, or wind energy. The first option – batteries, is very popular due to its simple structure and low cost but it needs maintenance in a short interval. Direct power source is very effective in the aspect of energy lifetime; but it is impractical in many cases with sensor deployment in rural areas or harsh environment. The supply from solar cell panels seems to be ideal but with increasing cost, maintenance and also depending on the weather of deployment areas. In Oklahoma, the solar solution for energy conservation is acceptable with 4 months of summer and other 8 months with medium sun-light. However, with strong winds, hail storms and

other type of harsh weather factors, solar panels need much maintenance and replacement. The power source from wind energy has been considered but until now there is no real application for sensors. With bridge structure, solar source can be a viable option for exposed sensors with reasonable budget and long life-time. In this project, we examined the advantages and disadvantages of each type of energy sources, and provide recommendations for SHM.

Phase 3 – Topology selection and topology control: Wireless sensor networks (WSNs) topology in simple meaning is the way that sensors are distributed in networks. The sensors in WSNs are not independent anymore; so the matter of topology is vital. Topology control is an iterative process with 2 phases of construction and maintenance running alternatively. In the topology construction phase, the optimal structure is constructed based on some criteria and lasts for a while for salability before going into maintenance phase. In the topology maintenance phase, some algorithms are used to monitor the networks. When the current topology is no longer optimal, the monitoring algorithm triggers a change to topology construction phase for a new optimal reduced topology. This process occurs iteratively during the lifetime of the WSNs.

WSN topology construction includes the following two major techniques:

- The **backbone-based** technique first creates a subset of nodes in the set of nodes in WSNs as the backbone for the networks, and then all other nodes in WSN must be able to directly connect to at least one of nodes in this backbone. The subset is created based on one popular mathematical problem called Connected Dominating Set (CDS) and optimization algorithm is applied to identify the Minimum Connected Dominating Set (MCDS).
- The **cluster-based** technique creates many groups of nodes called clusters and each cluster has a gateway node (cluster-head). Nodes in each clustered are selected based on common characteristics.

Phase 4 – Sensor network optimization: The optimal sensor network layout will seek a balance of the following criteria:

- **Coverage:** The coverage range is a trade-off with number of sensor nodes and energy reservation matter. A bridge includes many critical parts and these parts are not in small scales. Sensors are not cheap and the number of sensors used for WSNs for overall bridge structure damage detection is not a small one. In application field of SHM with the particularities of structures, the WSNs have to fully cover the critical parts to provide the best information about suspicious points.
- Power efficiency: the good communication modes can improve the lifetime of the sensors and networks due to minimized energy spending. The mixed modes of event-driven, time-driven and on-demand reporting in a consensus mechanism will save much energy for sensors and networks in limit sources of power.

Network communication capacity: the WSNs basic properties still depend on multi-hop communication so packet collisions are certainly common. To reduce the rate of internal collision between nodes communication, hybrid and optimal topology come to help with minimum domination set and clustered-based combined.

4.2 Design of wireless sensor network simulator for topology optimization

We simulated bridge damage detection (BDD) using a wireless sensor network (WSN) simulator. The purpose of the simulator is to allow users to upload pictures of bridges or critical parts of structures and control the deployment of different types (and number) of sensors. The simulator takes various inputs from the end-user allowing a greater degree of flexibility. It provides an optimal deployment of sensors based on the topology and optimization criteria selected.

As shown in Figure 4.1, the WSN simulator is modeled as a web-portal driven by an engine. The web-portal consists of 3 key components: Interface, Data Access, and Business Logic. A database is used to store and retrieve information via Data Access. We explain the functions of the simulator, other web pages and the role of each of the components as below.

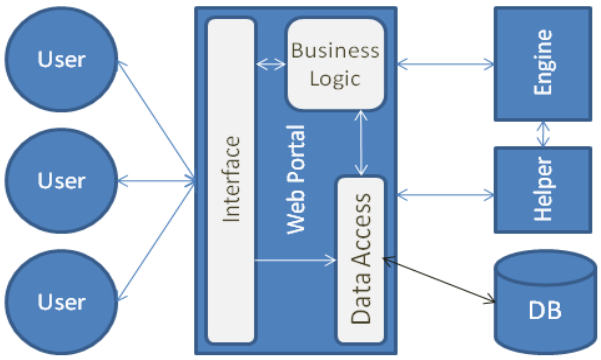

Figure 4.1 WSN simulation system main components

The Simulation System

The interface of the portal acts as the communication medium between the overall system and the end-user. The public user interface is where users can interact, control the deployment of sensors, run simulation and do other tasks. When users log on using their authenticated user names and passwords they are automatically taken to the *Home* page (main user interface of the simulator). It consists of 4 interactive sections as shown in Figure 4.2, namely, Image File, Sensor Configuration, Topology, and Control. It also consists of two additional sections: Tracking and Damage definition.

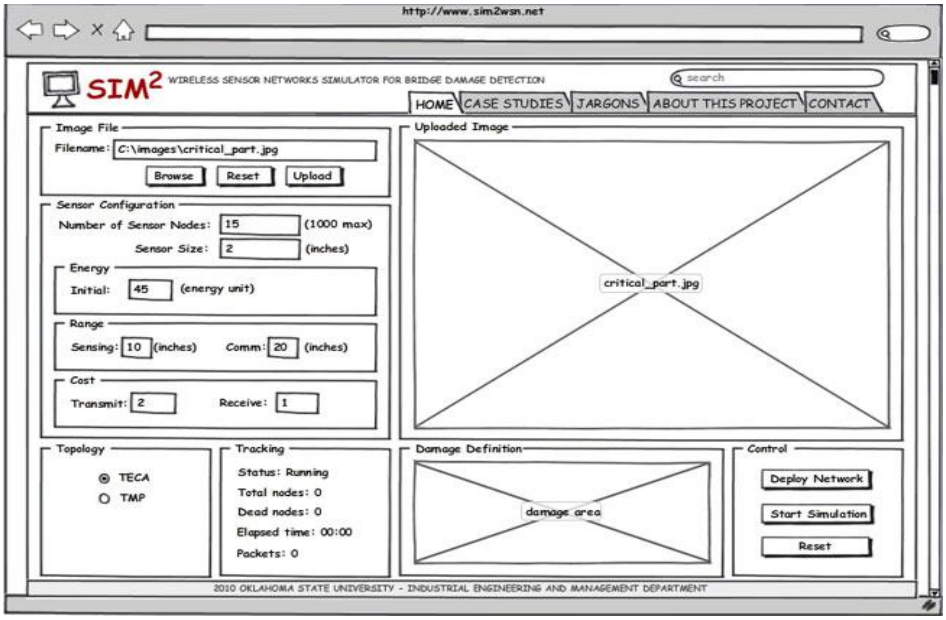

Figure 4.2 WSN Simulator Interface

Users choose an image of the structure (or critical part) they want to analyze and upload this in the Image File section. The simulator takes images with .jpg as the extension. Once the image is uploaded the user can view it on the screen (on the right hand side). By using the mouse the user can define damage boundaries interactively.

Sensor configuration helps the user select the number of sensor nodes, size of the sensor (in inches) to be deployed/tested, initial energy, coverage or range of the sensor, cost of packet transmission/reception. The number of sensor nodes defines the size of the network. The size is the radius of each sensor node in the network and battery life of the sensor is captured via initial energy input. Range or the coverage of the sensor includes the range of the transmission/reception and range of sensing of each sensor node. Cost per packet for each transmission and reception is also captured for the purpose of optimizing the performance of the system.

The third section, *Topology,* allows users to choose between two network topologies for optimizing sensor deployment. The topology of a network plays a key role in the performance of control algorithms in the network. In many cases, not all network links are needed for communication purposes. Identifying redundant and unnecessary topology information, usually referred to as topology management, can significantly improve the performance of ad hoc networks, and *sustain network operations over extended period of time*. Topology management has been effectively applied in ad hoc networks to supplement routing control protocols, and to schedule efficient channel access to propagate broadcast data.

Topology management in ad hoc networks is an approach to hierarchically organizing networks, and should be differentiated from *topology control through power control*. Both approaches can serve the energy efficiency and interference reduction purposes, critical for ad hoc wireless networks. However, power control mechanisms *save the energy consumption of individual nodes* and reduce mutual interference by adjusting the transmit power level on a per-node basis, so that one-hop neighbor connectivity is balanced and overall network connectivity is ensured.

The *tracking* section displays important information about status of the simulation and the user input. The WSN simulator allows the users to define their own damage area in the *damage definition* section. Finally, the *control section* consists of deploy network, start simulation and reset buttons which optimize the network using the topology configuration, start the simulation and reset the current run of the simulation, respectively.

Database: To store communication packet data, a database management system (Microsoft SQL Server Express 2008) is deployed. Data is stored as tables in the database and currently consists of the following tables: (1) *Users*, storing user management information such as user id and password, last accessed date, permission and description; (2*) Sessions*, stores session information for each user with fields such as session id, session start time, session end time and description; (3) *Images*, containing the images uploaded by each user, path to the image storage, size, quality, description and format type; (4) *Configurations*, containing the information of WSNs mentioned earlier such as transmit cost, receive cost, energy, number of sensors for each session, results of deployment and optimization, etc., and (5) *Other,* contains information about the rules for senor deployment, constraints and other miscellaneous information required or obtained during optimization.

4.3 Random field method for optimal sensor placement

A complete structural analysis to monitor health of a structure must include the *uncertainties associated with geometry of structure, type of loads, and material (of construction) properties*. Additionally, in order for the SHM system to detect with maximum probability any structural damage before it becomes critical, wireless *sensors* need to be *optimally placed*. While many advances have been made in terms of sensor technology, damage detection algorithms, structural reliability, and deterministic sensor placement optimization (SPO) schemes, much additional research needs to be focused on probabilistic modeling, probabilistic analysis and design, as well as on SPO under uncertainty, in order to *extract maximum information* about the structure's condition while taking the uncertainties into account.

To maximize the probability of detecting damage, an optimal deployment of sensors is necessary. However, *temporal and spatial variability* in parameters of an environment such as material, geometric, and loading factors need to be explicitly captured to make informative decisions. We propose a new integrated approach which aims at to maximize the probability of detecting corrosion over a given area on a structure (such as a concrete bridge or beam) by optimizing the number and locations of sensors considering spatial correlations among the different locations on the structure. These steps are described in detail in the subsequent sections.

4.3.1 Development of the framework

Figure 4.3 shows the overall Random Field (RF) framework in a simplistic manner. The sensor placement problem (including determining the number of sensors) is solved by using an optimization algorithm that has as its input: (1) the mechanical properties of the structure under consideration, and (2) Structural properties of the object under consideration.

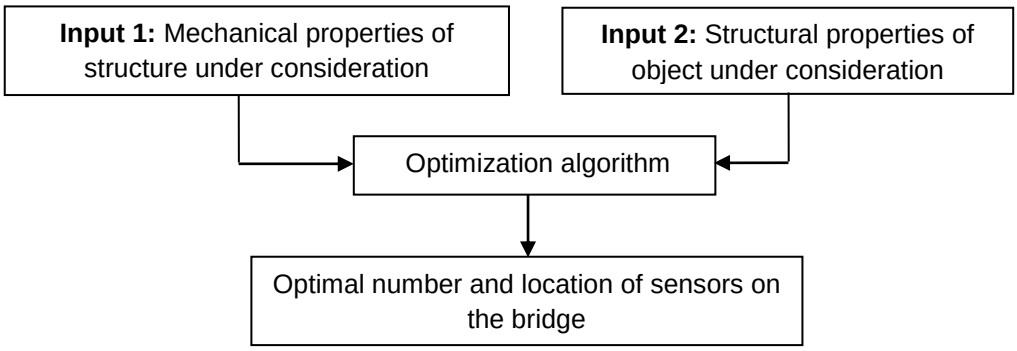

Figure 4.3 Flowchart for optimal sensor placement using random field method

Typically users will need to input some properties of the bridge known prior to the model since the random field method as well as the optimization procedure relies on the type of structure and its physical properties. Then the optimization algorithm minimizes the mean square error of the predictions at unmeasured points. The algorithm approach here is novel and simultaneously considers both mechanical and structural properties.

4.3.2 Advantages of the random field method

We would like to determine the predictions at *P* desirable locations of the structure (bridge, henceforth) given the response measurements at N locations and the correlation properties of the random mechanical load *and* the structural properties of corrosion diffusion. The response predictions are based on information provided from response measurements and the structural model while the corrosion properties are captured using a simple corrosion-diffusion approach. The accuracy of the predictions will depend on the locations and the number of sensors. The objectives are (a) to determine the best locations of a given number of sensors such that the predictions at the *P* unmeasured location involve the least error, and (b) to determine the number of sensors needed for the prediction error to be below a specified threshold. Random field method enables capturing spatial (and temporal) correlations in sensor measurement. Since corrosion diffusion exhibits both these properties i.e., corrosion spreads across the structure (spatial) and over time (temporal), we must place minimum required sensors at appropriate locations that will maximize the probability of detection of corrosion. In addition, it is clear that two sensors placed very close to each other will detect the same level of corrosion over time; and hence some minimal distance is required to place the sensors that maximizes the coverage area (in this case the bridge). Random field method captures this correlation structure and is an efficient tool that aids in optimization of sensor placement for SHM purposes.

4.4 Sensor placement optimization for SHM

This section addresses sensor placement optimization (SPO) for damage detection in multistory buildings. The sensor placement optimization problem is formulated using partial differential equation modeling and Fisher information matrix (FIM) based on the American Society of Civil Engineering (ASCE) benchmark structure [9].

The proposed methodology has the following advantages: (1) partial differential equation modeling of the benchmark structure is proposed to formulate the optimal criteria for the SPO damage detection problem. The dynamic characteristics of the underlying structure are accurately calculated using a closed form solution of the equivalent ordinary differential system. Moreover, instead of using partial differential

equations (PDEs) for each node in the Finite Element Method (FEM), displacement functions are used, which reduce the computational time with a satisfying accuracy; and (2) a multi-component objective function based on FIM is used to minimize the overall uncertainty of the estimated parameters.

Fisher Information Matrix (FIM) For Sensor Placement Optimization: According to Ref. [12], the FIM can be written as,

$$\mathrm{FIM} = \phi^{\mathrm{T}}\phi$$

Here, ϕ refers to the Jacobian matrix of the acceleration of the multistory structure with respect to each sensor location. The Jacobian matrix formulation is illustrated in Appendix A.4. Using the Singular Value Decomposition (SVD) [14], ϕ can be defined as,

$$\phi = \mathrm{USV}^{\mathrm{T}}$$

where, $\mathrm{U} \in \mathbb{R}^{\mathrm{m}\times\mathrm{m}}, \mathrm{V} \in \mathbb{R}^{\mathrm{n}\times\mathrm{n}}$ is an orthogonal matrix whose columns are left (right) singular vectors that define an orthonormal basis for the output sensor measurement space and for the input parameter space, respectively; and $\mathrm{S} \in \mathbb{R}^{\mathrm{m}\times\mathrm{n}}$ is a rectangular diagonal matrix with nonnegative real numbers on the diagonal called singular values σ.

The Objective Function: In this study, the objective function has three components. The first one is based on the determinant of FIM [9] which is the product of the singular values. The determinant of FIM has to be maximized since its inverse is a measure of the overall uncertainty on the estimated parameters. The second component of the objective function for the sensor placement is the trace of the FIM [9] defined as the sum of the singular values. The last component of the objective function is the condition number of the FIM which is defined as the ratio of the largest to the smallest singular value. Each of the previous metrics emphasizes on a specific aspect of the optimization problem. Thus, it is recommended to combine them in aggregated Figure of Merit (FOM), which should be maximized and can be expressed as [9],

$$\mathrm{FOM} = \mathrm{w}_1\ \mathrm{Det}\ + \mathrm{w}_2\ \mathrm{Tr}\ - \mathrm{w}_3\ \mathrm{CN}$$

where, CN, Tr and Det are the condition number, trace and determinant of the FIM, respectively; w_i are weighting factors between the components of the objective function.

Application to ASCE Benchmark Problem: This section uses the benchmark structure as a case study for the proposed optimal sensor placement methodology. Three different optimization algorithms, namely, Sequential Space Filling (SSF) [13], Genetic Algorithm (GA) [7], and the simulated annealing Algorithm (SA) [15] were adopted to optimize the final locations of the eight sensors.

After running each method thirty times and choosing the best results for each method, it has been found that the performance of the Simulated Annealing algorithm is the best in solving the sensor placement problem in the optimality of sensor location (See Figure 4.4).

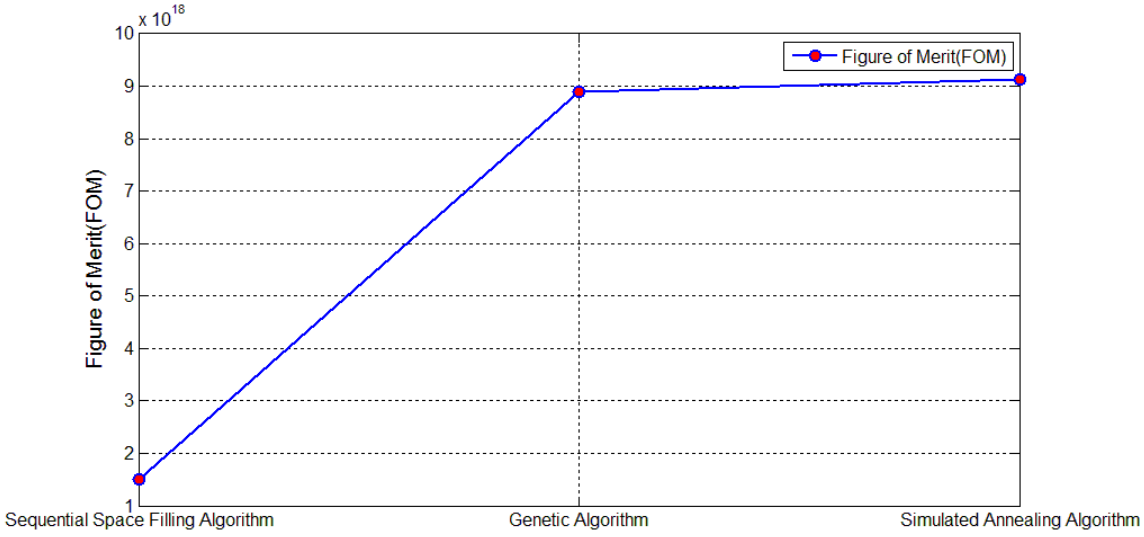

Figure 4.4 Performance comparison of the FOM for different optimization algorithms

Optimization Results and Discussion: A schematic of the benchmark structure is shown in Figure 4.5, where the locations of the existing sixteen sensors are indicated by circles (four sensors in each floor). Moreover, the 3D graphic random field of the objective function (Figure of Merit) for the fourth floor is shown in Figure 4.6.

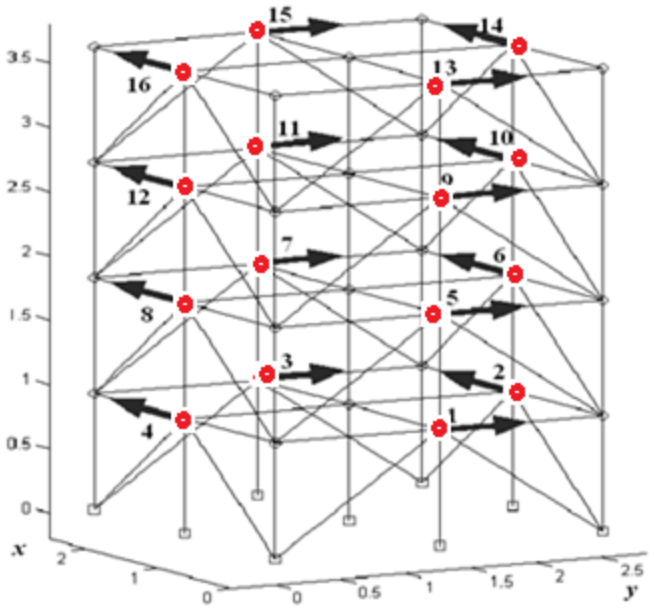

Figure 4.5 Existing placements of sensors on the ASCE benchmark structure [8]

In this section, the optimal sensor placement of the benchmark structure is studied using the simulated annealing algorithm (SA). Only eight sensor locations are needed and randomly selected as an initial input and a 0.98 of cooling factor is applied.

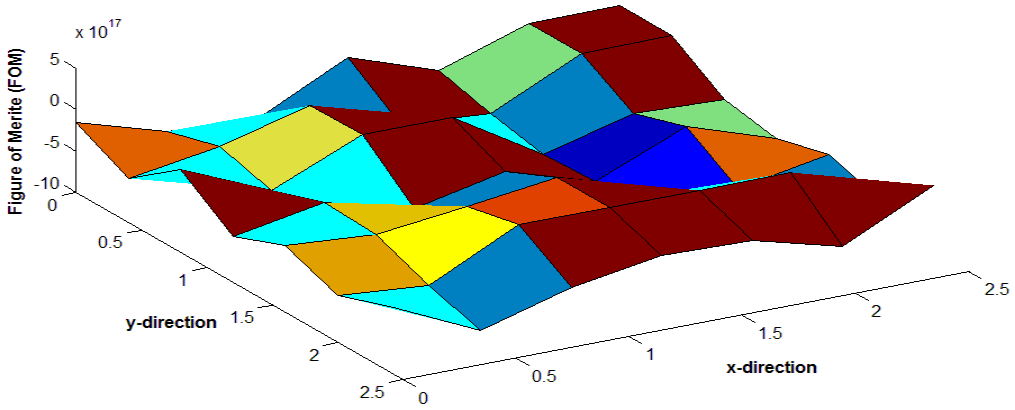

Figure 4.6 3D graphic random field for the fourth floor of the benchmark structure

Applying unit weights to each component of the FOM, the objective function of the FIM is computed as shown graphically in Figure 4.7. Moreover, the optimal sensor coordinates are given in Tables 4.1 and shown in Figure 4.8.

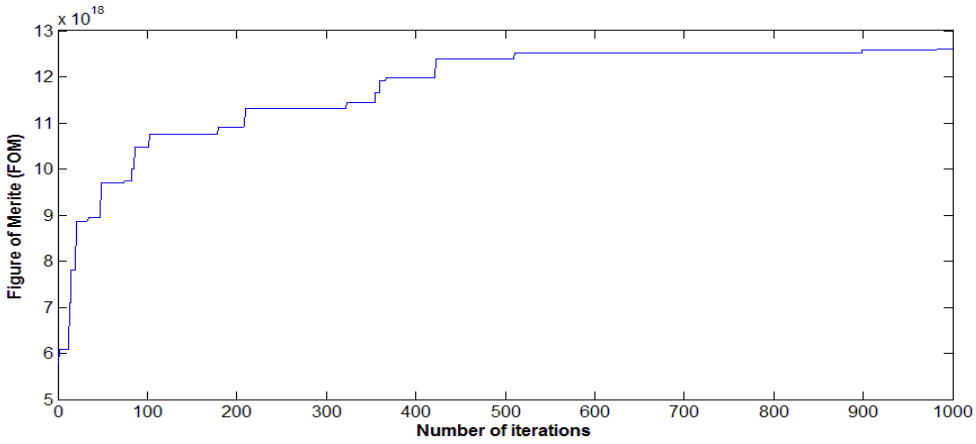

Figure 4.7 Figure of Merit using simulated annealing algorithm

Table 4.1 Optimal sensor coordinates based on the Figure of Merit

Sensor number	S_1	S_2	S_3	S_4
Coordinates	(0.0, 2.2, 0.9)	(2.2, 0.3, 0.9)	(0.1, 2.5, 1.8)	(0.2, 2.5, 1.8)
Sensor number	S_5	S_6	S_7	S_8
Coordinates	(0.6, 2.3, 2.7)	(2.5, 0.0, 2.7)	(2.4, 0.4, 3.6)	(0.7, 1.4, 3.6)

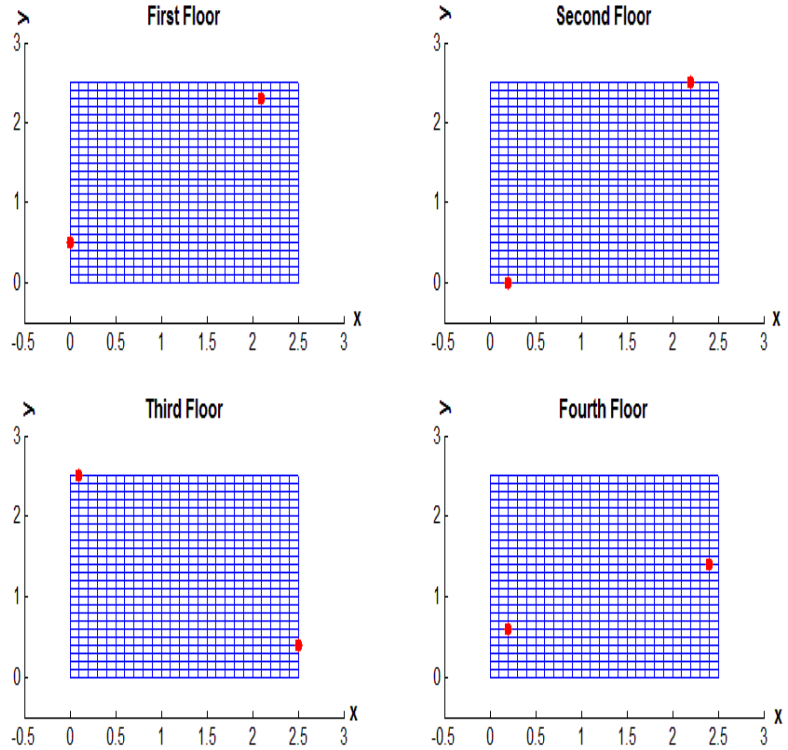

Figure 4.8 Optimal sensor locations for the four floors of the benchmark structure

Based on the optimization results, it is observed that the FOM values converge directly after 150 iterations with a maximum average value of 12.6×10^{18}. From Table 4.1, it can be seen that the optimal sensor locations are located near the boundaries of the benchmark structures. This result may be due to the nature of the bracing system placed diagonally on each floor of each exterior face. In fact, the removal of this bracing system is designed to simulate damage to the benchmark structure.

Capability of Damage Detection: In order to validate the efficiency of the selected optimal sensor sets using the simulated annealing algorithm, six damage patterns generated from the benchmark model, taken from Ref. [2]. Each test case is repeated forty times with different realization of measurement noise and the average of each test case is further investigated. In addition, the Hotelling T^2 multivariate control chart [8] for monitoring the mean vector of the process is used. The out-of-control average run length (ARL_1), which is the number of observations needed until the change is detected, was investigated for the sensor configuration of the benchmark structure before and after the optimization. The results of the comparison using ARL_1 as a performance measure are summarized in Table 4.2.

Table 4.2 ARL_1 results for the sensor configuration of the benchmark structure using Hotelling *T2* control charts for all six different damage patterns

Operating condition	**ARL_1 (before optimization)**	**ARL_1 (after optimization)**
Very slight damage	P 6: ARL_1= 10.6	P 6: ARL_1= 6.2
Patterns 6 and 3	P 3: ARL_1= 5.2	P 3: ARL_1= 3.1
Medium local damage	P 4: ARL_1= 2.6	P 4: ARL_1= 2.3
Patterns 4 and 5	P 5: ARL_1= 2.5	P 5: ARL_1= 2.0
Severe damage	P 1: ARL_1= 1.0	P 1: ARL_1= 1.0
Patterns 1 and 2	P 2: ARL_1= 1.0	P 2: ARL_1= 1.0

From Table 4.2, we noticed that, the Hotelling T^2 control chart after optimization has shorter ARL_1 than that before optimization except for the severe damage cases

(patterns 1 and 2); in other words, the Hotelling T^2 control chart captures the damage earlier using the optimized sensor locations.

Based on reported percentage loss in stiffness associated to each damage pattern shown in Table 4.3 [2], the power of damage detection occurred in the benchmark structure using the proposed SPO methodology can be quantified.

From Table 4.3, the proposed SPO methodology using the simulated annealing algorithm has the capability to differentiate between operating conditions with different levels of damage. In fact, the optimal sensor configuration has improved the detection performance in capturing all different levels of percent loss in structural stiffness, especially, the operating conditions with slight damage.

Table 4.3 Percent loss in stiffness associated to different damage patterns for the benchmark structure

Damage patterns	**D_0**	**D_1**	**D_2**	**D_3**	**D_4**	**D_5**	**D_6**
Percent loss in stiffness (Johnson et al., 2004)	N/A	30%	60%	5.6%	10.2%	11.3%	2.3%

5. Robust Statistical Process Control for SHM

The purpose of this task is to detect the damage of the structure based on advance statistical analysis and signal processing technologies using sensor data. The nature of this task requires very profound background in quantitative analysis, and we have obtained significant amount of field measurement data from an actual bridge structure, which makes the analysis possible.

The ARIMA time series modeling is applied to strain data obtained from an actual bridge structure. Spectral component analysis of the strain data is also carried out, which includes Fast Fourier transform, Wavelet analysis, Empirical Mode Decomposition, and Hilbert Huang Transform. The spectral component analysis of data obtained from Finite Element modeling of the bridge is investigated using Fourier and Wavelet transforms. The analysis of experimental data obtained from a bending fatigue response of grouted stay cables is performed.

An experimental threshold based on a normalized energy of each Intrinsic Mode Function (IMF) was developed to determine the number of relevant IMFs and those who were generated by numerical error. A modified Hilbert-Huang transform (MHHT) was developed in this task for damage detection. Comparative studies between the Modified Hilbert-Huang transform and continuous wavelet analysis was carried out for more effective structure damage identification. The computation of correlation dimension was also developed as an application in chaos theory and nonlinear time-series analysis for the purpose of structural health monitoring. Correlation dimension is used as features extraction to detect damage in bridge structures.

5.1 Time series modeling an actual bridge structure

This subsection summarizes the findings and data analysis results obtained from an actual bridge structure. The data is obtained from strain gauges mounted on the supporting columns of the bridge.

Data compression and feature extraction: Four strain gauges were mounted on two of the supporting columns of the bridge, namely column-Dd6 and column-H19C. Hourly

strain measurement data and temperature at each sensor location was obtained daily from each of the sensors with full year data obtained for 2002-2004 and partial data for 2001 and 2005. The full data set from 2002-2004 was utilized for analysis. Instead of the hourly strain data from each sensor, we used the daily average measurement. For each day the average of the four sensors was taken, which makes the number of data points to 365 points per year.

Analysis method used: A time series plot is fitted in Figure. 5.1 for the bridge column strain data. Y-axis represents strain data and X-axis is the time in the units of days. For time series analysis, Auto Regressive (AR), Moving Average (MA), and Auto Regressive Integrated Moving Average (ARIMA) can be applied [16]. However, from Figure 5.1, it can be seen that the strain data is not stationary which means the mean and/or variance of the data is changing over time. This makes it difficult to apply time series analysis directly. Therefore, some regression analysis is necessary to model the trend of the data before, time series analysis can be applied.

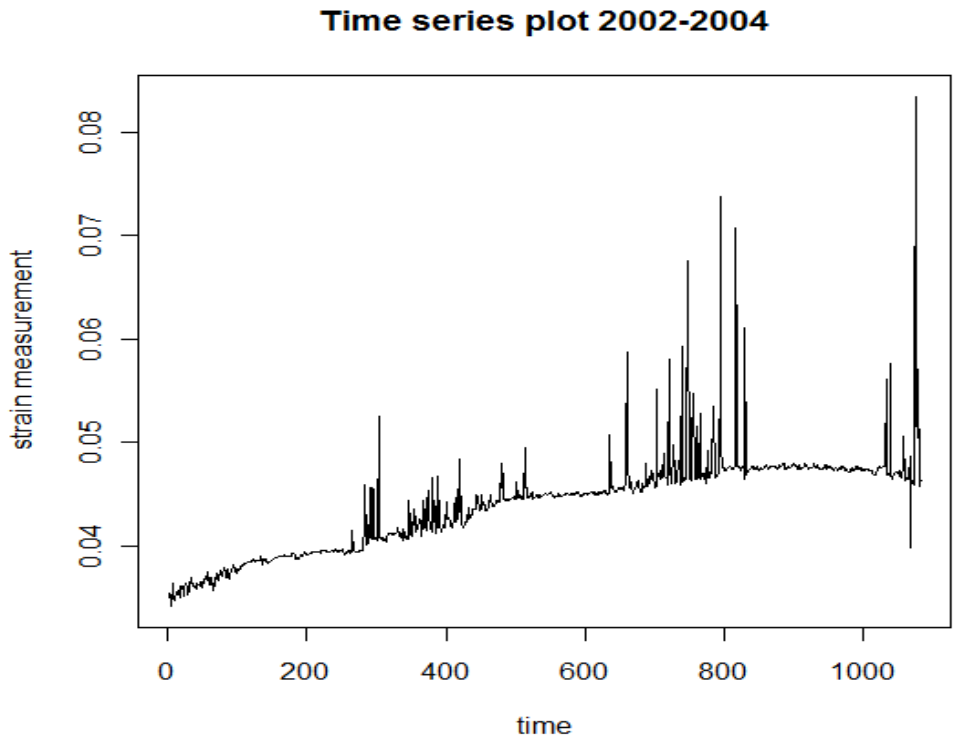

Figure 5.1 Time series plot of strain data for the year 2002-2004

Results obtained: Quadratic-regression curve is fitted for the whole time series data with R^2 value of 95% (Fig. 4.2). This means that 95% of the data can be explained or represented by the quadratic equation given as:

$$Y(t) = -6.726e\text{-}008(t^2) + 3.509e\text{-}005(t) + 0.03495$$

where Y represents the strain measurement values, and t represents time.

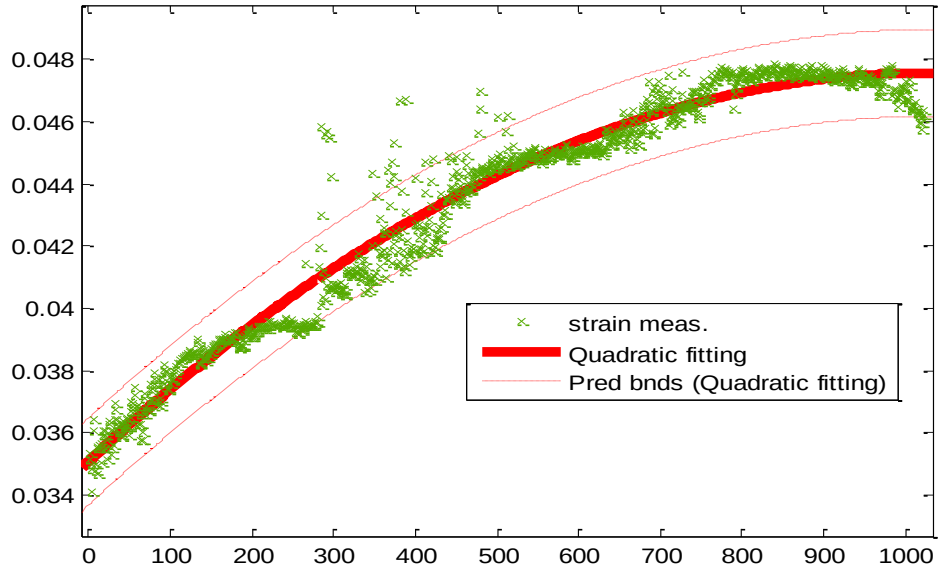

Figure 5.2 Quadratic-regression curve fitted for the strain data from 2002-2004

After the above regression model is obtained, the difference between the model and actual data, namely, the residuals are used for time series analysis, such as ARIMA model fitting. The order of C(0,1,2) is used, and the following model was obtained.

$$Y(t)= -0.7097w_{t-2} - 0.0975\ w_{t-1} + w_t$$

The order for the ARIMA model is obtained by plotting the auto correlation function (ACF) and partial auto correlation function (PACF) for the residuals. Based on this ARIMA model for the residuals and the fitted regression model for the trend, we are able to forecast future values of the strain data.

Conclusion: The model for the time series data contains two parts. The first one is fitting a quadratic regression equation for the original data set and the second part is fitting ARIMA with order C (0, 1, 2) for the residuals. Using these two models, the strain

data in the future can be forecasted. By continuously running these two models, we can utilize the resulting coefficients of the ARIMA model to construct statistical control charts for monitoring abnormalities in the data, which may correspond to damage.

5.2 Spectral component analysis for bridge data

Spectral component analysis, such as Fourier transformation and Wavelet analysis, is applied to sensor data. The original time series data plotted in Figure 5.3 is de-noised using wavelet transform to obtain its approximation and detail coefficients. The original signal can be represented by the approximation signal and the details are considered as noise.

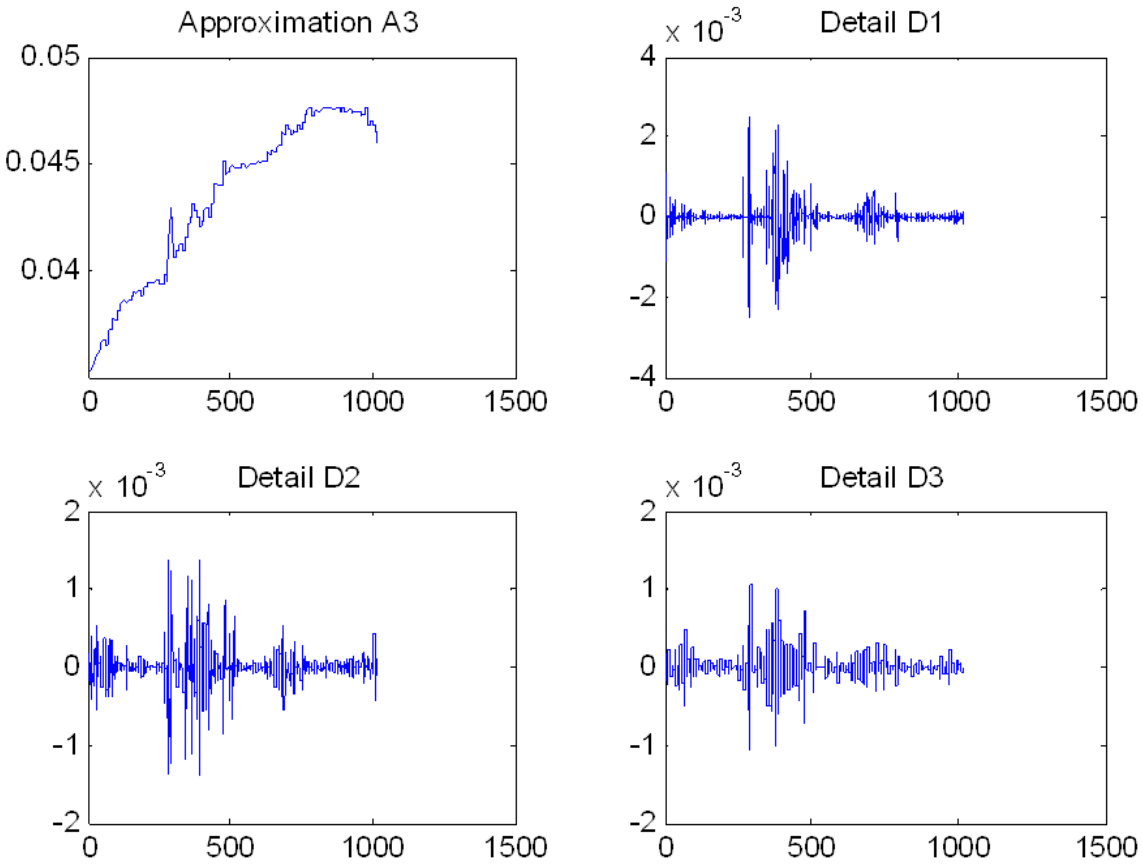

Figure 5.3 Wavelet analysis of the original signal

5.3 Hilbert transform analysis for bridge data

A very important and related topic with Hilbert transform is empirical mode decomposition (EMD). EMD is an effective approach to decompose the data into a collection of intrinsic mode functions (IMF), based on which the Hilbert analysis can be applied [10].

IMF by definition is any function with the same number of extrema and zero crossings, with its envelopes, as defined by all the local maxima and minima, being symmetric with respect to zero. The Hilbert transform and instantaneous frequency analysis for the sensor data measured from an actual bridge structure are shown in Figure 5.4, which delineates the IMF components of the time series data. It has 6 IMF components and the last one (the one at the bottom of Figure 5.4) is the residual. Y and X axes represent strain and time, respectively, but within different bandwidth modeled by IMFs.

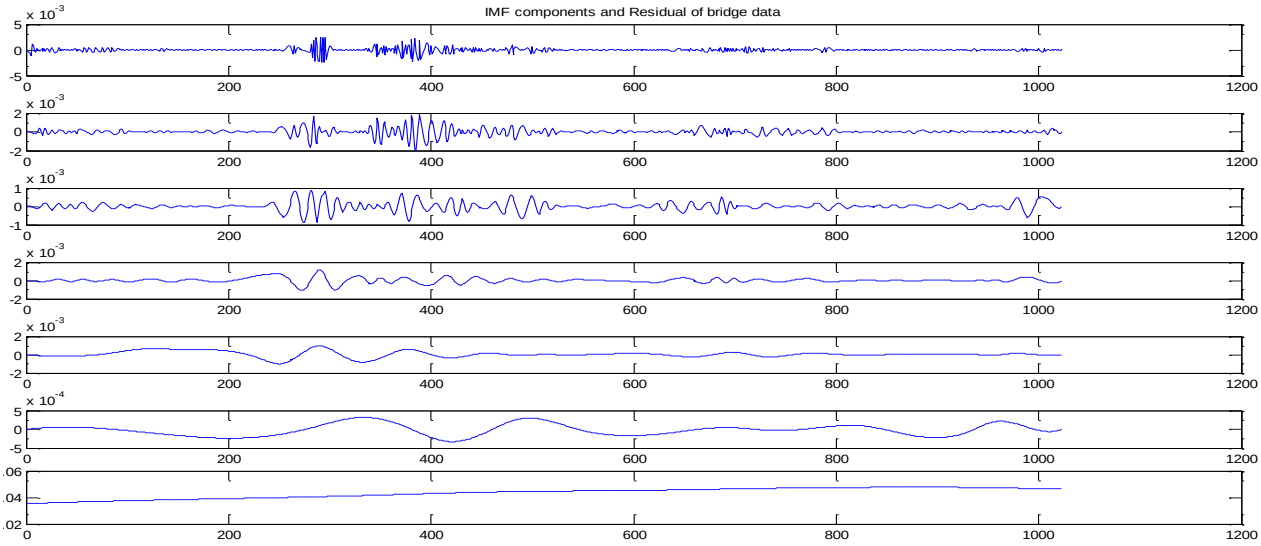

Figure 5.4 EMD analysis of an actual bridge structure

5.4 Analysis of data from a lab test specimen of stay cables

The primary objective of this sub-task was to investigate the bending fatigue response of grouted stay cables. Both the Fred Hartman and Veterans Memorial bridge have been experiencing large amplitude cable vibration. A major concern resulting from these vibrations is the possibility of fatigue damage to the parallel, seven-wire, pre-stressing strand in the grouted stay cables – and the overall safety of the bridges.

Conclusion: The most critical regions for fatigue damage are the ends of the stays and locations where dampers and restrainers are connected to the stays. Reducing the amplitude of the displacements had the largest influence on increasing the fatigue life of grouted stay cables of the parameters studied. Approximately 95% of the wire breaks that were identified in the laboratory tests were caused by fretting fatigue. Fretting is a special wear process that occurs at the contact area between two materials under load and subject to slight relative movement by vibration or some other force; and the risk of this type of fatigue damage can only be reduced by reducing the amplitude of the vibrations.

5.5 Comparative study for analyses of bridge data

This part introduces a modified Hilbert Huang Transform (MHHT) and compares it with continuous Wavelet analysis for structure damage identification. The capabilities, effectiveness, and accuracies of these two techniques are compared by using acceleration measurement simulation data from benchmark problem established by the ASCE Task Group on Structural Health Monitoring, which provides a platform for consistent evaluation [2] and allows various aspects of the Structural Health Monitoring problem to be controlled for a better understanding of the effectiveness and sensitivities of these methods.

Data compression and feature extraction: The bench mark structure from which simulation data was taken is a 2.5 m by 2.5m floor area and 3.6 m high. A bracing system placed along the diagonal was fixed for each bay to emulate a real structure, a concrete slab was built at each floor and the removal of these braces is designed to simulate damage to the structure. The experiment wind ambient excitation and another two types of forced excitation sources were introduced. Impact hammer test and electrodynamics shaker was applied for the forced excitation case [3]. One undamaged case and six damage patterns were the subject of study of this benchmark problem considering damage patterns simulated.

Instantaneous frequency and energy spectrum are used as feature extraction in Modified Hilbert Huang Transform (MHHT), while Wavelet coefficients with Morlet function are used in Wavelet analysis.

Methodology: (a) Four different cases were created to test the validity of the frequency domain approaches. The first one is data obtained from the undamaged state of the structure by applying the default parameters of the Matlab^{TM} program. The second case is obtained by running the simulation for damage pattern-2, which removes all the braces from the 1st and 3rd floor. The third case considered is data from damaged condition but with a less damage extent (pattern-1) simulated by removing the braces on the 1st floor. The fourth case is the combination of damaged (pattern-2) and undamaged conditions of the bench mark structure. The sampling frequency taken for all the different cases is 1000Hz, and the time span of the simulation is 40 sec. (b) To support and validate choosing the specific threshold to select the relevant IMFs, the signal was analyzed with a one –way between subjects ANOVA, where subjects were nested in IMFs.) and Dunnett T3 test (2-sided with 99% confidence interval) as a post hoc analysis was conducted. The Instantaneous frequency of each IMFs was randomly assigned and the normality assumption was valid. The homogeneity of variance assumption was tested empirically using Levene test.

Results obtained: Result of conducting a one –way between subjects ANOVA ($F(4, 145)=33.465$, p-value $=0.0001$) was statistically significant F-test, which supported choosing the specific threshold to select the relevant IMFs.

The intrinsic physical property of the original data is clearly reflected using IMFs; on the other hand, Wavelet coefficients are strongly influenced by the selected mother wavelet. Also, the energy distribution with time and frequency is presented more clearly using Hilbert spectrum than using Morlet spectrum, so the HHT is more capable of accurately determining the time instant when the damage occurs regardless of the noise level.

Conclusion: The comparison results indicate that MHHT presents more accurate detailed characters of time history signal and sensitive damage detection technique, as it has better resolution both in the time domain and in the frequency domain, which can

be beneficial to establish a robust signal processing approach for the development of effective and efficient structural health monitoring (SHM) system.

5.6 Correlation dimension for bridge data

Introduction: This part focuses on the computation of correlation dimension as an application in Chaos Theory and nonlinear time-series analysis for the purpose of structural health monitoring.

Data Compression and Feature Extraction: Acceleration measurement simulation data from benchmark problem established by the ASCE Task Group on Structural Health was generated. The real data was obtained from deformation gauges mounted on the supporting columns of an active bridge.

Correlation dimension as an application in Chaos Theory and nonlinear time-series analysis was used as feature extraction for the purpose of structural health.

Methodology: An attractor based analysis techniques a long with invariant measures were placed in the context of damage detection.

After reconstructing the attractor set in state space from the deformation raw time series, the data can be quantified using different kinds of dimension. The correlation dimension is the most popular measure of dimension. Because its calculation is relatively fast, simple and it gives a deeper understanding of the underlying dynamical system. Moreover, it has an operational and more rigorous mathematical definition which provides a G-P algorithm to deal with not only experimental time series data, but also simulation data [4].

The correlation dimension is the most popular measure of dimension. It is derived from the correlation sum, which is “a cumulative correlation function that measures the fraction of points in the *m*- dimensional reconstructed space and is defined as

$$C\ r,m\ = \frac{2}{n_m\ n_m-1} \sum_{i,j=1,j>i}^{n_m} \Theta\ r - \ x\ i,m\ - x\ j,m \quad ,$$

where Θ is the Heaviside function, such that $\Theta\ x\ = 0\ if\ x \leq 0\ and\ \Theta\ x\ = 1\ for\ x > 0,$, ... indicates the Euclidean norm of the vector, $N_m = N - \ m - 1\ \tau$.

The correlation dimension is defined as follows:

$$D_2 = \lim_{r \to 0} \log C\ r, m\ / \log r$$

where D_2 is the correlation dimension, $C\ r, m\ $ is the correlation sum. The linear scaling region from the log-log of $C\ r, m\ $ versus *ln*(*r*) is measured. Finally, plot the correlation dimension D_2 versus embedding dimension, which is the obtained value for the plateau zone [5].

Discussion: The state space reconstruction and the correlation dimension plots of analyzed simulation signals and real sensor data are presented in Fig. 4.5.

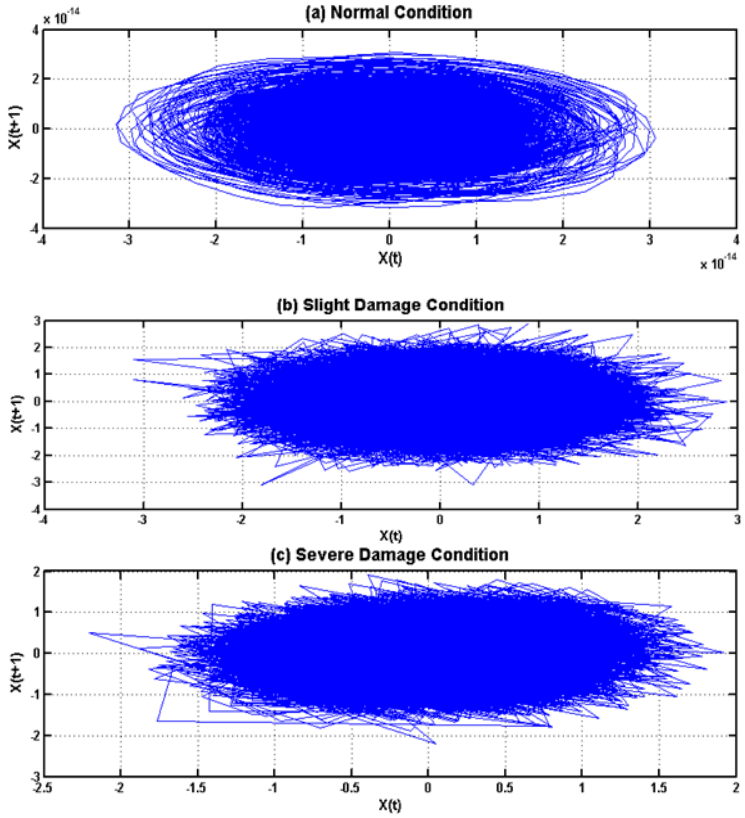

Figure 5.5 Attractor reconstruction for different running conditions

The computation procedure starts with choosing the right time delay, then computing the correlation sum for each of successively larger embedding dimension for different radii r. After that, the correlation sum versus radius, which defines a separate relation for each embedding dimension, is plotted.

The first stage of nonlinear time series analysis is to reduce noise level from the sensor measurements data using only the related Intrinsic Mode Functions from the Empirical Mode Decomposition. After noise reduction, an attractor reconstruction technique, which includes choosing the right time delay and the right embedding, is followed. Figure 5.5 shows the state space reconstruction of acceleration measurement simulation data for different operating conditions: normal undamaged condition, minor damage and severe damage. From the state space reconstruction plots, it is applicable to distinguish between normal undamaged case and other damaged cases, because the attractor plots for the damaged cases look more irregular. However, it is hard to distinguish between levels of damage using only state space reconstruction plots because the attractor plots only qualitatively displays geometric features of the state space projection and cannot indicate any quantitative character [6]. On the other hand, the correlation dimension is able to provide quantitative information about the underlying process.

Based on the above state space reconstruction techniques and using the G-P algorithm, the correlation dimension of the signals in both case studies (simulation data from benchmark problem and the real data of an active bridge) is shown in Figures 5.6 and 5.7, respectively, while the computational results are summarizes in Tables 5.1 and 5.2, respectively.

Table 5.1 Correlation dimensions with different operating conditions

Data length	Operating condition	Computed correlation dimension
30000	Undamaged condition	D2=3.45
30000	Slight damaged	D2=3.12
30000	Severe damaged	D2=2.86

Table 5.2 Correlation dimensions of bridge strain data with different years

Data length	Operating condition	Computed correlation dimension
7000	First year (2002)	D2=4.69
7000	Third year (2004)	D2=3.34

The correlation dimension value for the normal running condition in study case one is 3.45, which is higher than that of the other two damaged scenario. During the damage testing process, the correlation dimension decreases as more braces were removed. Looking at sensor real data in case study two, the correlation dimension value is 4.69 in 2002 and it has decreased to 3.34 in 2004 which could be an indicator of the existence of damage to the bridge structure.

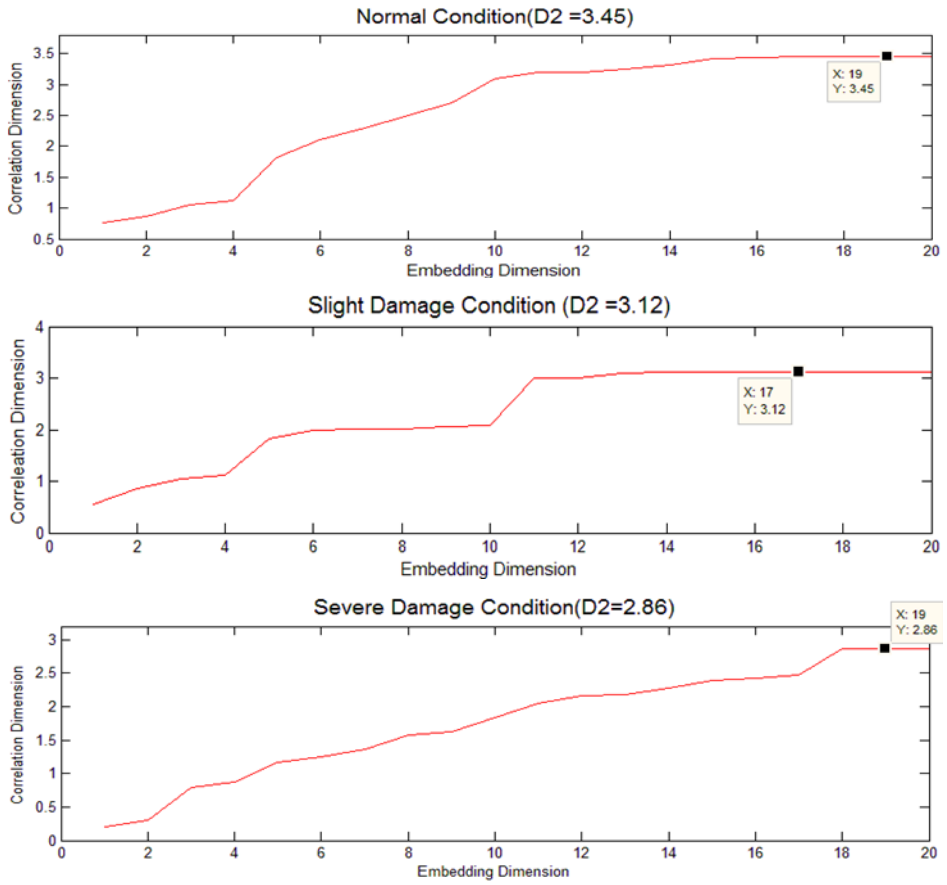

Figure 5.6 The correlation dimension of simulation signals in different conditions

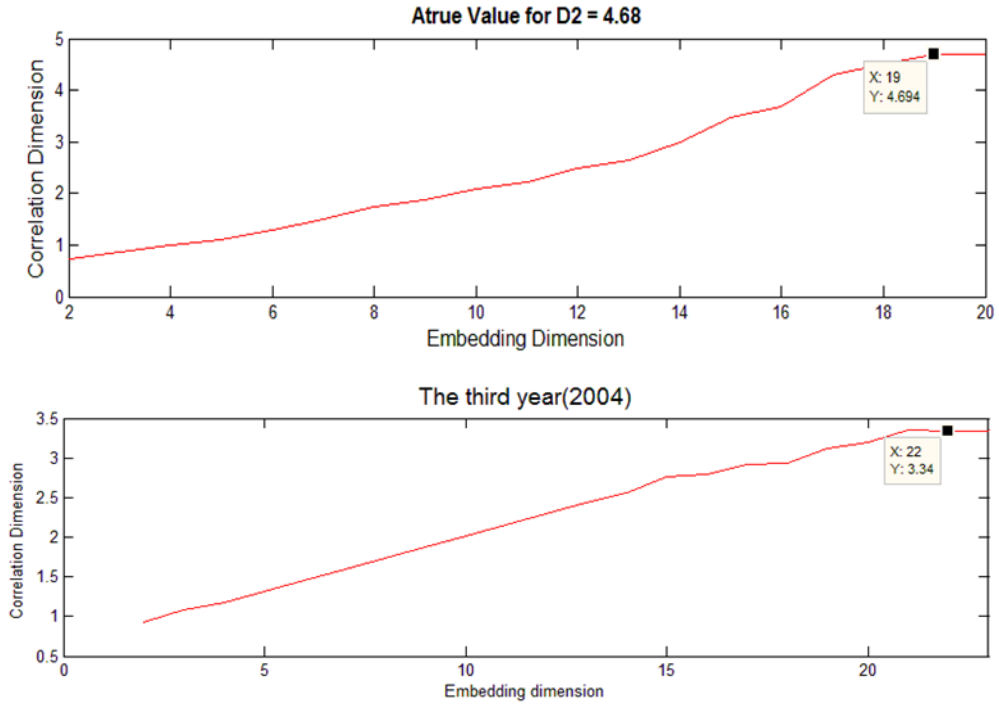

Figure 5.7 The correlation dimension of real sensor signals in different years

Conclusion: Non-linear time series analysis technique based on the application of correlation dimension in bridge's structure damage detection is introduced. Results of applying the correlation dimension to simulation data show that the correlation dimension can provide some intrinsic information on an underlying dynamic system. Also it has the capability to distinguish between operating condition with slight damage or severe damage compared with the normal undamaged condition. Moreover, the obtained results from a real world sensor data demonstrate that the correlation dimension could be used as feature extraction to detect damage in bridges.

5.7 Damage prediction using empirical mode decomposition

To track structural integrity and ensure safe and reliable systems, an effective predictive model based change point detection to predict the severity of civil infrastructural damage is important. In this study, an online prediction method for analyzing the nonlinear and nonstationary signals based on local empirical mode decomposition and the locally weighted linear predictor is developed.

5.7.1 The proposed methodology

An illustration of the proposed hybrid damage prediction methodology is given in Figure 5.8.

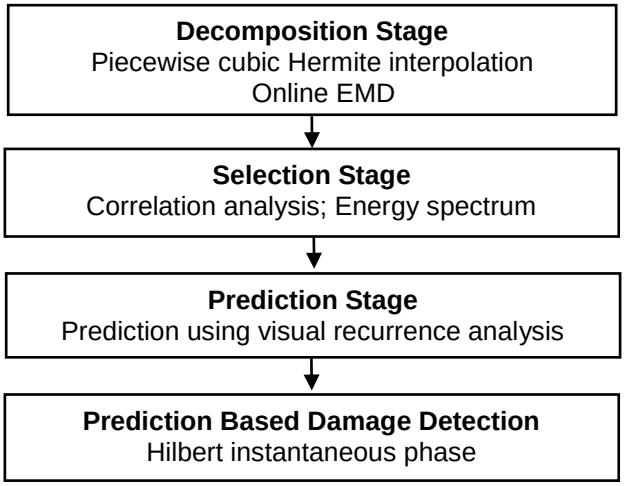

Figure 5.8 The overall damage prediction methodology

In this section, an effective online monitoring method for the nonlinear and nonstationary signals based on local empirical mode decomposition is presented. We proposed a local implementation of the standard empirical mode decomposition using a sliding window of flexible length, and thus the sifting process will be conducted by blocks enabling the Hilbert Huang transform to be used as an effective online analysis technique. EMD provides a number of IMFs and for the purpose of online structural health prediction, it is so important to select the most appropriate and representative one. In this study, statistical correlation analysis between the original signal and each IMFs, as well as the normalized energy of each IMF will be used to identify the best appropriate IMF. In fact, the final selection criterion has at least two IMFs with a highest normalized energy. In this study, the instantaneous phase of each IMF is used as a monitoring statistics of statistical control charts for change point detection. In fact, the control charts in the multiple chosen IMFs can be constructed independently due to the property of the EMD, i.e., the spaces of IMFs are nearly orthogonal to each other. Thus, univariate control charts are applied for each individual IMFs, instead of multivariate control charts.

5.7.2 Case study: structure damage prediction using Hilbert instantaneous phase

To validate the proposed method in predicting the severity of different damage patterns at relatively high levels of noise, the proposed method is applied to a benchmark structure, which was designed by the American Society of Civil Engineers (ASCE) for the application of SHM [2].

Decomposition Stage: To demonstrate the capability of the Hilbert instantaneous phase for structure damage prediction, a series of signals are constructed by combining the undamaged state of the ASCE benchmark structure and the damaged state. The reconstructed signal has information of the time when the damage occurs with different damage patterns. The initial windowed signal length was chosen to be 1850 data points with a sliding window of 20 data points to satisfy a minimum value of R^2 of approximately 0.6.

Selection Stage: According to the results of the correlation analysis of each selected IMF along with the normalized energy, the second and the fourth intrinsic mode functions were chosen as the best representative of the original windowed signal for the purpose of further prediction analysis. The proposed selection criterion eliminates the first IMF, which contains most of the signal's noise [10].

Prediction Stage: The second and the fourth IMFs time series of the initial windowed signal will be used as an input for the locally weighted predictor with the following parameters: Gaussian Kernel and Euclidean distance. The bandwidth that controls the size of the neighborhood in which the nearest neighbors are sought has found to be 15. Moreover, the prediction horizon is chosen to be 20, which is still less than the number of zero crossings of the chosen IMF that represent the effective prediction horizon [11].

Validation of the Proposed Predictor: To test its performance on the most representative IMFs, the proposed locally weighted linear predictor is compared with different prediction techniques such as exponential smoothing, stepwise autoregressive and ARIMA. Specifically, the prediction accuracy has been tested using the Mean Absolute Percent Error (MAPE) and R^2, whereas, Variance of Absolute Percentage

Error (VAPE) is used to test the prediction stability [1]. The results of the comparison are summarized in Table 5.3.

The results from the comparison in Table 5.3 reveal that the proposed method has achieved the highest R2 and less MAPLE and VAPE, thus it outperforms the other three models in terms of prediction accuracy and stability.

Table 5.3 Prediction comparison for the first windowed signal over twenty forecasting steps ahead

Model	MAPE (%)	R^2	VAPE (%)
Exponential Smoothing	9.29	0.218	0.81
Stepwise Autoregressive	8.47	0.473	0.63
ARIMA	11.13	0.115	1.12
Proposed Method	6.91	0.56	0.47

Damage Prediction: After validating the accuracy and stability of the locally weighted linear predictor, we keep calculating the Hilbert instantaneous phase, which extends linearly over time for the most representative IMFs (both the second and the fourth IMFs) until a slope change in the Hilbert phase is detected outside the upper and lower threshold. It should be pointed out that the threshold is chosen experimentally to be 4% of the original slope of the Hilbert phase. The slope change in the Hilbert phase occurs at the time where the travelling wave meets the structure's damage. As soon as the wave passes the structural damage, the slope of the damaged phase behaves as the undamaged slope. Thus, the Hilbert phase for the second and fourth IMFs will be simultaneously predicted. In this case study; there is an early change in the Hilbert phase outside the threshold band for the fourth IMF in the fifth sliding window at time step equal to 1933 as demonstrated in Figure 5.9 and a more zoomed one in Figure 5.10.

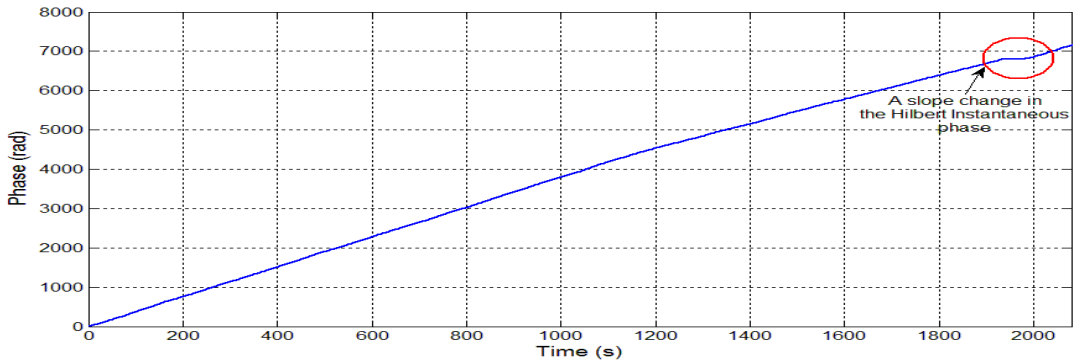

Figure 5.9 Hilbert instantaneous phase for the fourth IMF including the predicted damage point

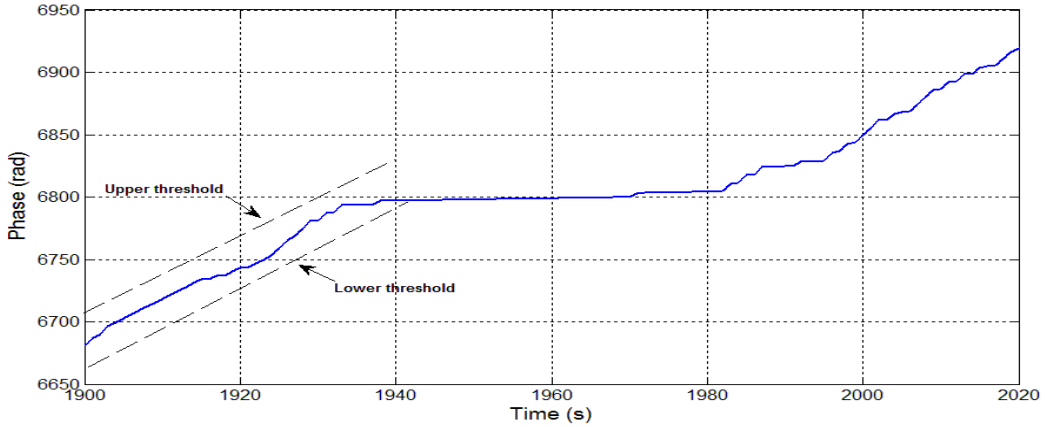

Figure 5.10 Zooming window of Hilbert instantaneous phase for the fourth IMF

From Figure 5.10, it is clear that the predicted change point is occurred at time step equal to 1933, which means that the damage is predicted to occur after 3 seconds delay. Each simulation has been replicated 30 times to ensure the accuracy of the predicted time delay.

Performance Evaluation: The performance evaluation of the proposed damage detection method is demonstrated using mean time delay and compared with wavelet analysis at different levels of noise as shown in Table 5.4 and Table 5.5.

Table 5.4 Comparison results between the proposed method and Morlet wavelet for the data with low level noise (NSR of 5%) for six different damage patterns

Operating condition	Mean delay (MWC)	Mean delay (the proposed method)
Very slight damaged Patterns 6 and 3	P 6: τ= 16.21 P 3: τ= 3.35	P 6: τ= 13.72 P 3: τ= 3.01
Medium locally damaged Patterns 4 and 5	P 4: τ= 1.88 P 5: τ= 1.85	P 4: τ= 1.04 P 5: τ= 1.03
Severe damaged Patterns 1 and 2	P 1: τ= 1.29 P 2: τ= 1.27	P 1: τ= 1.06 P 2: τ= 1.02

Table 5.5 Comparison results between the proposed method and Morlet wavelet for the data with high level noise (NSR of 20%) for six different damage patterns

Operating condition	Mean delay (MWC)	Mean delay (the proposed method)
Very slight damaged Patterns 6 and 3	P 6: τ= 168.81 P 3: τ= 143.74	P 6: τ= 42.1 P 3: τ= 27.62
Medium locally damaged Patterns 4 and 5	P 4: τ= 22.51 P 5: τ= 14.98	P 4: τ= 6.3 P 5: τ= 6.7
Severe damaged Patterns 1 and 2	P 1: τ= 3.11 P 2: τ= 3.19	P 1: τ= 2.07 P 2: τ= 2.05

The comparison indicates clearly that the proposed damage detection method do outperform the WEWMA control charts. In other words, it captures the damage earlier than the Morlet wavelet based damage feature, especially with a very slight damage and high level of noise.

Damage Severity Prediction: To predict the damage severity of the benchmark structure, the proposed quantitative relative energy index (REDI) is compared with the percent loss in stiffness of the 12-DOF models as shown in Table 5.6. The comparison

indicates that the proposed prediction method captures the loss in stiffness of the structure, and thus effectively differentiates the normal condition with different levels of damage.

Table 5.6 Comparison between the proposed relative energy damage index and percent loss in stiffness of 12 degree of freedom shear-building models

Damage patterns	1	2	3	4	5	6
REDI (Representative IMF)	20.32%	34.60%	2.93%	5.37%	5.19%	0.71%
Percent loss in stiffness [2]	30%	60%	5.6%	10.2%	11.3%	2.3%

In this case study, the existence of damage of the underlying dynamic system is accurately detected using the slope change of the Hilbert instantaneous phase of the most sensitive IMF within all candidates, after trying them all simultaneously. The severity of structural damage is predicted using the energy of the predicted part of the selected IMF.

In this subtask, an efficient methodology for prediction based change point detection has been developed for online structural health monitoring (SHM). Within each adaptive sliding window, the proposed method performs the sifting process in the EMD using piecewise Hermit interpolation. The EMD based online prediction applies the locally weighted linear predictor and consists of two steps: (1) change point detection using Hilbert instantaneous phase; (2) and damage severity prediction using the energy index of the most representative IMF. The case study indicates that: (1) the proposed boundary distortion processing method for EMD has achieved a significant reduction in the boundary effects; (2) moreover, the damage existence of the underlying dynamic system is accurately detected with a minimum time delay using the slope change of the Hilbert instantaneous phase; and (3) it is also demonstrated that the proposed relative energy damage index (REDI) based on the energy changes of the selected IMF has the capability to effectively predict different levels of damage.

6. Summary and Conclusion

In this project, the research tasks and the corresponding outcomes are summarized as follows,

(5) **Case studies for SHM of bridges**: 40 different case studies of the use of structural health monitoring for different types of transportation infrastructure have been compiled and summarized. These case studies are useful for providing some guides for civil engineers with respect to what kind of sensors and analysis tools could be chosen for different types of bridges. For each bridge, the following questions are investigated and answered: (i) General information about the bridge; (ii) Types of sensor used and measured parameters; (iii) What are the key areas of measurement? (iv) What utilities are available? (v) What accuracy is needed in the measurement? (vi) What rate of readings is needed? (vii) How will the data be retrieved? (viii) How was the data processed? and (ix) What challenges did the project have?

(6) **Critical damages identification of bridges using Finite Element Modeling**: This task is focused on the structural modeling of a bridge using finite element modeling. Two simplified computational models have been developed to confirm the capability of replicating a field load test. The models are updated to more closely present the actual field test data. Additional details are added to more closely resemble the as-built and field conditions of the bridges. These models can also be used to identify critical areas on these bridges to determine potential locations for sensor placement in a structural health monitoring.

(7) **Optimal sensor placement for Structural Health Monitoring**: The basic methodology and procedure for bridge sensor network are investigated, such as (1) sensor selection, (2) choice of power source, (3) sensor network topology design, and (4) sensor location optimization criteria. This task formulates the optimal criteria of the sensor placement optimization for damage detection problem based upon a partial differential equation (PDE) analytical model. The PDE model is derived and then validated through experimental results. The study results show that the proposed optimal sensor placement method minimizes the uncertainty in

the estimated model parameters, leading to reduced number of sensors and improved detection rate for structural damages;

(8) **Application of advanced statistical analysis and signal process techniques**: These tools have been applied to monitor the structural health condition of bridges. (a) The ARIMA time series modeling is applied on strain data obtained from an actual bridge structure. Spectral component analyses of the strain data is also carried out, which include Fast Fourier transform, Wavelet analysis, and Empirical Mode Decomposition (EMD) and Hilbert Huang Transform (HHT). Among these methods, the EMD and HHT show their superior performance for early damage detection; (b) correlation dimension is used as features extraction to detect damage in bridges. The proposed damage detection algorithm using correlation dimension can significantly alleviate the complexity of computation, making the online monitoring of nonlinear/nonstationary processes more applicable and efficient; and (c) the proposed empirical mode decomposition method for online damage prediction overcomes the boundary effects and has significant prediction accuracy improvement over other commonly used prediction techniques.

The technology transfer activities from this project are summarized as follows,

(1) Attended the Second Annual OKTC Summer Symposium, with a poster titled "Development of a Structural Health Monitoring (SHM) Guidebook for Critical Bridge Structures," at TBIP Oklahoma City, on July 29, 2011.

(2) Attended ODOT-OKTC Transportation Research Day, with a poster titled "Development of a Structural Health Monitoring (SHM) Guidebook for Critical Bridge Structures," at ODOT, on Oct. 11, 2011.

(3) Attended 2012 IIE (Institute of Industrial Engineers) Annual Conference, and presented the paper titled "A Quasi-Recursive Correlation Dimension Analysis for Online Structural Health Monitoring (SHM)" that was accepted by the conference proceeding, May 21, 2012, Orlando, FL.

(4) Attended the First Annual Heartland Transportation Consortium Student Competition (Mr. Mahmoud Mistarihi), with an oral presentation titled “A hybrid Modified Hilbert Huang Transform and Locally Weighted Linear Prediction Scheme for Online Structural Health Monitoring (SHM),” Renaissance Oklahoma City Convention Center Hotel, on April 3, 2013.

References Cited

[1] Zheng, W., Lee, D.-H., and Shi, Q., "Short-term freeway traffic flow prediction: Bayesian combined neural network approach," *Journal of Transportation Engineering,* vol. 132, pp. 114-121, 2006.

[2] Johnson, E., Lam, H., Katafygiotis, L., and Beck, J., "Phase I IASC-ASCE structural health monitoring benchmark problem using simulated data," *Journal of Engineering Mechanics,* vol. 130, pp. 3-15, 2003.

[3] Zhu, B., Leung, A., Wong, C., and Lu, W., "On-line health monitoring and damage detection of structures based on the wavelet transform," *International Journal of Structural Stability and Dynamics,* vol. 8, pp. 367-387, 2008.

[4] Wang, W., Chen, J., Wu, X., and Wu, Z., "The application of some non-linear methods in rotating machinery fault diagnosis," *Mechanical systems and signal processing,* vol. 15, pp. 697-705, 2001.

[5] Pai, P.F., Huang, L., Hu, J., and Langewisch, D.R., "Time-frequency method for nonlinear system identification and damage detection," *Structural Health Monitoring,* vol. 7, pp. 103-127, 2008..

[6] Grassberger, P., Schreiber, T., and Schaffrath, C., "Nonlinear time sequence analysis," *International Journal of Bifurcation and Chaos,* vol. 1, pp. 521-547, 1991.

[7] Guo, H., Zhang, L., Zhang, L., and Zhou, J., "Optimal placement of sensors for structural health monitoring using improved genetic algorithms," *Smart materials and structures,* vol. 13, p. 528, 2004.

[8] Montgomery, D.C., *Introduction to statistical quality control*, Wiley, pp. 491-510, 2007.

[9] Borguet, S. and Léonard, O., "The Fisher information matrix as a relevant tool for sensor selection in engine health monitoring," *International Journal of Rotating Machinery,* vol. 2008, 2008.

[10] Huang, N.E., Shen, Z., Long, S.R., Wu, M.C., Shih, H.H., Zheng, Q., Yen, N.-C., Tung, C.C., and Liu, H.H., "The empirical mode decomposition and the Hilbert spectrum for nonlinear and non-stationary time series analysis," *Proceedings of the Royal Society of London. Series A: Mathematical, Physical and Engineering Sciences,* vol. 454, pp. 903-995, 1998.

[11] Sa-ngasoongsong, A. and Bukkapatnam, S.T., "Willingness-to-pay Prediction Based on Empirical Mode Decomposition," in *Industrial Engineering Research Conference, Reno, NV*, 2011.

[12] Kammer, D. and Yao, L., "Enhancement of on-orbit modal identification of large space structures through sensor placement," *Journal of Sound and Vibration,* vol. 171, pp. 119-139, 1994.

[13] Huang, W., Kong, Z., and Chennamaraju, A., "Robust design for fixture layout in multistation assembly systems using sequential space filling methods," *Journal of computing and information science in engineering,* vol. 10, no. 4, 041001, 2010.

[14] Klema, V. and Laub, A., "The singular value decomposition: Its computation and some applications," *Automatic Control, IEEE Transactions on,* vol. 25, pp. 164-176, 1980.

[15] Tong, K., Bakhary, N., and Kueh, A., "Optimal Sensor Placement for Structural Health Monitoring Using Improved Simulated Annealing," in *Australasian Structural Engineering Conference 2012: The past, present and future of Structural Engineering*, 2012, p. 321.

[16] Shumway, R.H. and Stoffer, D.S., *Time series analysis and its applications: with R examples*. pp. 84-165, 2011: Springer.